



Faculty of Energy Technology

# Journal of ENERGY TECHNOLOGY



Volume 10 / Issue 1

MARCH 2017

[www.fe.um.si/en/jet.html](http://www.fe.um.si/en/jet.html)



Journal of  
ENERGY TECHNOLOGY



**VOLUME 10 / Issue 1**

Revija Journal of Energy Technology (JET) je indeksirana v bazah INSPEC© in Proquest's Technology Research Database.

The Journal of Energy Technology (JET) is indexed and abstracted in database INSPEC© and Proquest's Technology Research Database.



# JOURNAL OF ENERGY TECHNOLOGY

## Ustanovitelj / FOUNDER

Fakulteta za energetiko, UNIVERZA V MARIBORU /  
FACULTY OF ENERGY TECHNOLOGY, UNIVERSITY OF MARIBOR

## Izdajatelj / PUBLISHER

Fakulteta za energetiko, UNIVERZA V MARIBORU /  
FACULTY OF ENERGY TECHNOLOGY, UNIVERSITY OF MARIBOR

## Glavni in odgovorni urednik / EDITOR-IN-CHIEF

Jurij AVSEC

## Souredniki / CO-EDITORS

Bruno CVIKL  
Miralem HADŽISELIMOVIĆ  
Gorazd HREN  
Zdravko PRAUNSEIS  
Sebastijan SEME  
Bojan ŠTUMBERGER  
Janez USENIK  
Peter VIRTič  
Ivan ŽAGAR

## Uredniški odbor / EDITORIAL BOARD

**Zasl. prof. dr. Dali ĐONLAGIĆ,**

Univerza v Mariboru, Slovenija, predsednik / University of Maribor, Slovenia, President

**Prof. ddr. Denis ĐONLAGIĆ,**

Univerza v Mariboru, Slovenija / University of Maribor, Slovenia

**Doc. dr. Željko HEDERIĆ,**

Sveučilište Josipa Jurja Strossmayera u Osijeku, Hrvatska / Josip Juraj Strossmayer  
University Osijek, Croatia

**Prof. dr. Ivan Aleksander KODELI,**

Institut Jožef Stefan, Slovenija / Jožef Stefan Institute, Slovenia

**Prof. dr. Milan MARČIČ,**

Univerza v Mariboru, Slovenija / University of Maribor, Slovenia

**Prof. dr. Greg NATERER,**

University of Ontario, Kanada / University of Ontario, Canada

**Prof. dr. Enrico NOBILE,**

Università degli Studi di Trieste, Italia / University of Trieste, Italy

**Prof. dr. Brane ŠIROK,**

Univerza v Ljubljani, Slovenija / University of Ljubljana, Slovenia

**Doc. dr. Luka SNOJ,**

Institut Jožef Stefan, Slovenija / Jožef Stefan Institute, Slovenia

**Prof. dr. Mykhailo ZAGIRNYAK,**

Kremenchuk Mykhailo Ostrohradskyy National University, Ukrajina / Kremenchuk Mykhailo Ostrohradskyy National University, Ukraine,

#### **Tehnični urednik / TECHNICAL EDITOR**

Sonja Novak

#### **Tehnična podpora / TECHNICAL SUPPORT**

Tamara BREČKO BOGOVČIČ

#### **Izhajanje revije / PUBLISHING**

Revija izhaja štirikrat letno v nakladi 150 izvodov. Članki so dostopni na spletni strani revije - [www.fe.um.si/si/jet.html](http://www.fe.um.si/si/jet.html) / The journal is published four times a year. Articles are available at the journal's home page - [www.fe.um.si/en/jet.html](http://www.fe.um.si/en/jet.html).

Cena posameznega izvoda revije (brez DDV) / Price per issue (VAT not included in price): 50,00 EUR

Informacije o naročninah / Subscription information: <http://www.fe.um.si/en/jet/subscriptions.html>

#### **Lektoriranje / LANGUAGE EDITING**

Terry T. JACKSON

#### **Oblikovanje in tisk / DESIGN AND PRINT**

Fotografika, Boštjan Colarič s.p.

#### **Naslovna fotografija / COVER PHOTOGRAPH**

Jurij AVSEC

#### **Oblikovanje znaka revije / JOURNAL AND LOGO DESIGN**

Andrej PREDIN

#### **Ustanovni urednik / FOUNDING EDITOR**

Andrej PREDIN

Izdajanje revije JET finančno podpira Javna agencija za raziskovalno dejavnost Republike Slovenije iz sredstev državnega proračuna iz naslova razpisa za sofinanciranje domačih znanstvenih periodičnih publikacij / The Journal of Energy Technology is co-financed by the Slovenian Research Agency.



## ***Spoštovani bralci revije Journal of energy technology (JET)***

Energija je za sodobnega človeka izjemnega pomena. Prav zato se študij energetike uvršča med najbolj zanimive in perspektivne. Lahko rečemo, da je energetika (energija), poleg medicine (zdravja) in agronomije (prehrana), osnovna dejavnost, ki jo bo človeštvo vedno potrebovalo.

S fizikalnega stališča je pojem energije kompleksen. Z energijami in njihovimi pretvorbami se ukvarjajo mnogi raziskovalci na področju energetike. Na področju energetike se prepletajo znanja s področij strojništva, elektrotehnike, ekonomije, nanotehnologij, kemije, prava ... in prav zaradi interdisciplinarnosti je študij zanimiv.

Številni problemi, ki jih moramo rešiti za učinkovito izrabo energij, so večplastni. Analitične rešitve v takšnih primerih niso možne, zato se poslužujemo numeričnih izračunov in sofisticiranih numeričnih programov, s pomočjo katerih lahko v energetiki rešujemo probleme. Tudi ta tematika je obravnavana v tej številki.

Jurij AVSEC  
odgovorni urednik revije JET

## ***Dear Readers of the Journal of Energy Technology (JET)***

For contemporary society, energy is of utmost importance; therefore, studies of energy are among the most interesting and complex. Energy technology (energy) accompanied by medicine (health) and agronomy (food) are and always will be principal activities of human society.

From the physics point of view, the concept of energy is highly complex; the science of energies and their transformations employ many energy technology researchers. The energy sector combines knowledge from the fields of mechanical engineering, electrical engineering, economics, nano-technology, chemistry, law, and others. It is a fascinating interdisciplinary field.

Many problems need to be solved for energy efficiency, some of which are highly complex. Analytical solutions in such cases are not possible, so sophisticated numerical calculations are used. A number of sophisticated programs for the complex problems of the energy sector have been developed. This issue of JET examines this topic.

Jurij AVSEC  
Editor-in-chief of JET

# ***Table of Contents / Kazalo***

<b>Numerical Analysis of an Ahmed Body with Different Software Packages</b> Numerična analiza Ahmedovega telesa z različnima programskima paketoma <b>Simon Muhič, Matej Štefanič . . . . .</b>	<b>11</b>
<b>Critical analysis of formulae for the calculation of the electrical parameters of humid material</b> Kritična analiza formule za izračun električnih parametrov vlažnosti materiala <b>Borys Nevzlin, Valentyna Zagirnyak, Vitaliy Dziuban . . . . .</b>	<b>23</b>
<b>Optimization of Maintenance of Gensets Using Expert Systems for Fault Diagnosis</b> Optimizacija vzdrževanja generatorskih enot z uporabo ekspertnega sistema za diagnosticiranje napak <b>Željko Hederić, Dejan Barešić, Venco Čorluka . . . . .</b>	<b>35</b>
<b>Influence of Shading on I-V Characteristics of Thin film PV Modules</b> Vpliv senčenja na I-U karakteristiko tankoplastnih fotonapetostnih modulov <b>Matej Žnidarec, Danijel Topić, Josip Bušić . . . . .</b>	<b>47</b>
<b>Grounding system testing using a low voltage U-I method - some practical issues</b> Testiranje ozemljitve z uporabo nizkonapetostne U-I metode – praktična vprašanja <b>Ivan Tolić, Vedran Angebrandt, Ivana Hartmann Tolić . . . . .</b>	<b>59</b>
<b>Instructions for authors . . . . .</b>	<b>71</b>

# NUMERICAL ANALYSIS OF AN AHMED BODY WITH DIFFERENT SOFTWARE PACKAGES

## NUMERIČNA ANALIZA AHMEDOVEGA TELESA Z RAZLIČNIMA PROGRAMSKIMA PAKETOMA

Simon Muhič<sup>✉</sup>, Matej Štefanič<sup>1</sup>

**Keywords:** Computational Fluid Dynamics, Ahmed Body, Numerical analysis, Ansys Fluent, SolidWorks Flow Simulation

### **Abstract**

In this article, the results of CFD simulations are compared using two different software packages for numerical fluid dynamics. The analysis is performed for an Ahmed body, for which the measurement results and a variety of numerical simulations are available in the literature. The results of the stationary CFD simulations with the RANS approach show a significant difference between the results obtained with the SolidWorks Flow Simulation 2014 software and ANSYS Fluent 16.2 software in the air flow analysis area from 10 m/s to 60 m/s. The difference in computational time is also apparent.

### **Povzetek**

V članku primerjamo rezultate CFD simulacij, pridobljene s pomočjo dveh različnih programskih paketov za numerično dinamiko tekočin. Analiza je izvedena za Ahmedovo telo, za katerega so v literaturi na voljo tako rezultati simulacij, kakor tudi meritev. Rezultati CFD simulacij kažejo na signifikantno razliko med rezultati, ki smo jih pridobili s programsko opremo SolidWorks Flow Simulation 2015 in s programsko opremo ANSYS Fluent 16.2 v analiziranem območju toka zraka od 10 m/s do 60 m/s.

<sup>✉</sup> Corresponding author: Simon Muhič, Faculty of Technologies and Systems, Na Loko 2, SI-8000 Novo mesto, Slovenia, Tel.: +386 7 393 019, E-mail address: [simon.muhic@fts-nm.si](mailto:simon.muhic@fts-nm.si)

<sup>1</sup> Faculty of Technologies and Systems, Na Loko 2, SI-8000 Novo mesto, Slovenia

## 1 INTRODUCTION

CAE (Computer Aided Engineering), which refers to the extensive use of computer software to assist in engineering tasks and analyses, is increasingly evolving in engineering practice. It includes software for the analysis of solids using the method of finite element analysis (FEA), followed by software for analyses in the field of numerical fluid dynamics (Computational Fluid Dynamics (CFD)), electromagnetics, as well as coupled physics. The CAE software can also include add-ons to automatically optimize the analysed products. Analyses are very important in the development of products for achieving a better product quality. Engineers perform the analyses in the early development stage, where a virtual prototype of the product is made; after that, it is analysed and, if necessary, optimised to obtain the most optimal product which is sent to the production process. Certainly for virtual engineering, high-performance software that enables such analyses and high-performance computers for the processing of numerical data are both necessary. Such product development makes the development process cheaper and enables the company to be more competitive due to a shorter time for the development to the final product to be sent to the market. CFD analyses cover various analysis areas, from aerodynamics, combustion, heat transfer, chemical reactions, to many other areas where problems can be solved by numerical simulations of fluid mechanics. The software can be independent or, as recently common, in the form of an addition to 3D modellers. Therefore, the question that often arises is what software to choose. Due to the popularity of the high-performance software in the field of CFD, ANSYS Fluent on one side, and the prevalence of the CAD software SolidWorks enabling CFD analyses through its Flow Simulation interface, on the other, we opted for a direct comparison between the two software packages. Several analyses have been made, and the results do not show significant discrepancies between them, [1, 2].

For a direct comparative analysis, we performed an analysis of the Ahmed body, which was tested in the 1980s, [3]. The analysis was performed using the ANSYS Fluent and SolidWorks Flow Simulation software. We analysed the prediction accuracy as well as the speed of the software in solving the model. For the basic comparison, we compared the results of drag coefficient and lift coefficient. Figure 1 shows the Ahmed body for which the numerical analyses were performed. The body has a simple form on which the basic aerodynamic characteristics can be established, and several numerical analyses have been performed on it, such as [4, 5, 6, 7].

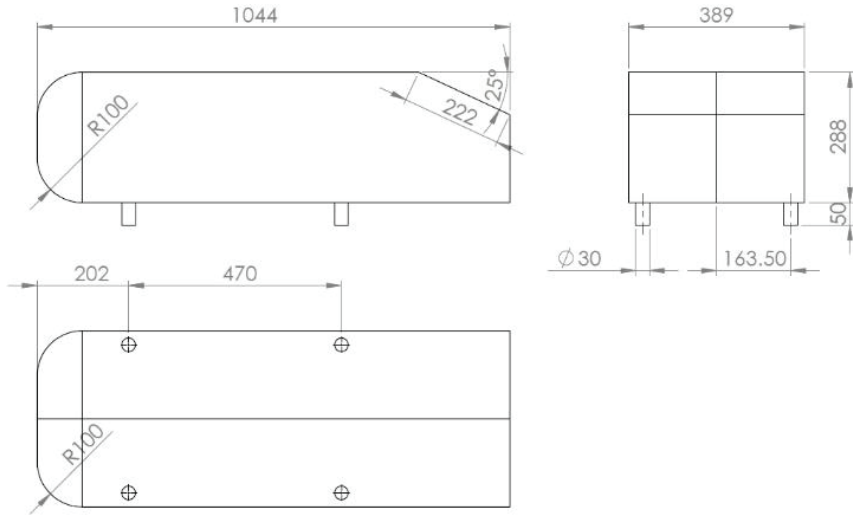


Figure 1: Ahmed body

The Ahmed body drag coefficient  $C_D$  in dependence on Reynolds number is given in the equation 1 [4]. The equation is obtained by the statistical analysis of the experimental data.

$$C_D = 0.2788 + 0.0915 \cdot e^{\left(\frac{-Re \cdot 10^{-6}}{1.7971}\right)} \quad (1.1)$$

## 2 VEHICLE AERODYNAMICS

Vehicle aerodynamics influences fuel consumption, vehicle stability, aerodynamic drag and the resulting noise. Drag force  $F_D$  acts in the opposite direction of the vehicle's movement, in the vehicle's direction. The first part of the force results from aerodynamic drag according to the form of the vehicle, the second part acts as a result of friction between the vehicle's surface and fluid which surrounds the vehicle. Figure 2 shows the action of forces on the vehicle.

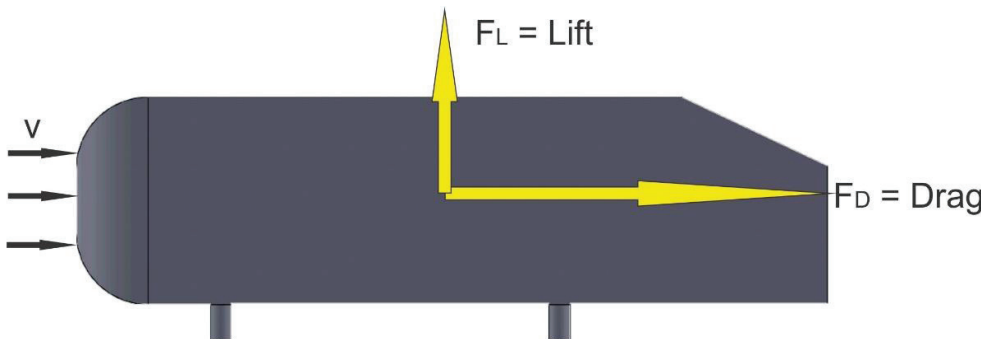


Figure 2: Forces on the Ahmed body, [8]

Drag coefficient  $C_D$  is the ratio between the drag force and dynamic force defined by the equation:

$$C_D = \frac{F_D}{p_d A} \quad (2.1)$$

As the surface  $A$  we consider the complete front head part, the dynamic pressure  $p_d$  being defined by velocity in front of the body. Similarly, lift coefficient  $C_L$  is defined with the equation:

$$C_L = \frac{F_L}{p_d A} \quad (2.2)$$

In this case, lift force  $F_L$  acts on the vehicle due to the surrounding air flow and the velocity difference between the lower and upper part of the vehicle.

### 3 NUMERICAL MODEL

For the numerical model, the RANS modelling approach was used. For modelling turbulence in the ANSYS Fluent software, the Realizable k- $\epsilon$  model (RKE) was used. To obtain boundary layers, the Enhanced Wall Treatment wall function was selected; it makes the k- $\epsilon$  model more suitable for treatment in the wider use of the non-dimensional variable  $y^+$ . In addition to the aforementioned model, the Non-Equilibrium wall function model, recommended for analysis in aerodynamics, was also used, [9]. The demand for the convergence value was that the residuals are less than 0.0005. The COUPLED scheme and the second order solvers were used. Numerical domain in the ANSYS Fluent software was divided into 12 volumes, allowing more types of numerical mesh and a better control of the individual parts of the domain (**Figure 3**).

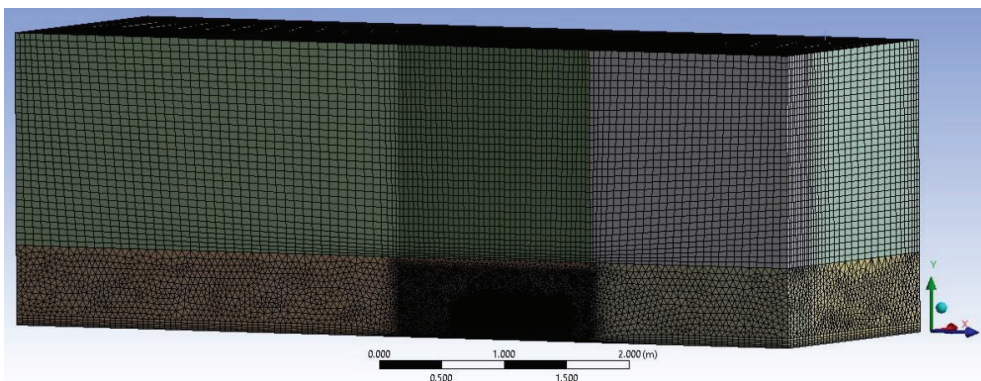


**Figure 3:** Numerical mesh in ANSYS Fluent

In the volumes above the body, a hexahedral mesh was used; around the body, however, a tetrahedral mesh was generated. In doing so, to obtain the boundary layers, we used the Inflation function on the model, allowing us to properly host the mesh on the walls (Figure 4).

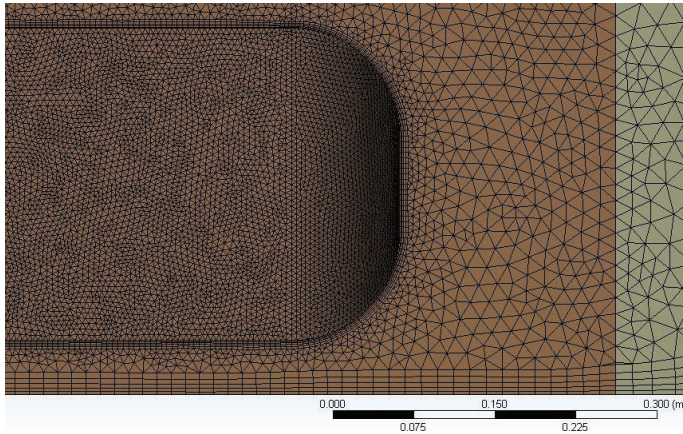


**Figure 4:** Detail of numerical mesh near Ahmed body

In the SolidWorks Flow Simulation software for modelling turbulence, the  $k-\epsilon$  turbulence model was also used. For wall function, the Two scale Wall Function was used, which essentially offers a similar solution as the Enhanced Wall Treatment setting in the ANSYS Fluent software. The convergence value was set on automatic. SolidWorks Flow Simulation uses only Cartesian mesh (Figure 5). Using the software tools, an additional meshing of the volume was performed around the body (Local Mesh Sizing). Several analyses were performed using a variety of meshes for finding a solution that is independent of the computational mesh. In addition, an analysis with adaptive mesh technology for the inflow velocity of 40 m/s was performed, the maximum number of cells was limited to 6000000 with a triple level of adaptation. A periodic adaptation of every 50 iterations was also used. For other analyses and velocity between 10 m/s and 60 m/s, the adaptive meshing was turned off.

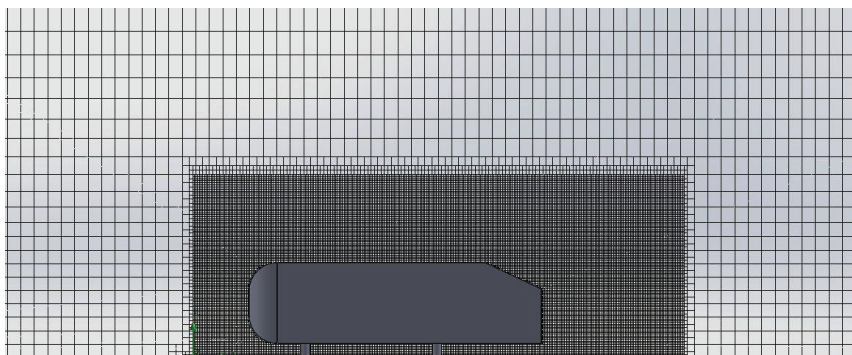


**Figure 5:** Numerical mesh in SolidWorks

## 4 NUMERICAL DOMAIN AND BOUNDARY CONDITION

The numerical domain was large enough to obtain a free flow, without the impact of domain walls to the geometry analysis. The size of domain analysis was specified for both analyses in accordance with the recommendations, [8]. In dealing with the problem, we decided for the analysis with respect to the plane of symmetry, since the software packages allow such approach. The Velocity Inlet was given as a boundary condition, in which we were changing the incoming velocity between 10 and 60 m/s on one side of the domain; on the other side of the domain, we used the Pressure Outlet boundary condition, where a pressure outlet without gauge pressure (0 Pa) was set. Air density during the analysis was 1.225 kg/m<sup>3</sup>, dynamic viscosity 1.7965 E-5 kg/(m s), and the surrounding pressure 101325 Pa. The analysis was performed for an incompressible fluid and isothermal conditions.

## 5 RESULTS

### 5.1 Referential example

**Table 1** shows the results of the numerical analysis at the referential air inflow velocity of 40 m/s and measurements, [4]. It can be seen that in the analysis with ANSYS Fluent software using the Realizable k- $\epsilon$  turbulence model with Non-Equilibrium walls treatment (Fluent RKE-NEQ) the aerodynamic drag coefficient deviates from the measured value by -0.1%, the lift coefficient deviates by 1.9%. The variable  $y^+$  on the walls of the body in this instance was  $y^+_{min} = 3.5$ ,  $y^+_{max} = 115$  in  $y^+_{ave} = 60$ .

A larger deviation, however, can be found in the results using the software SolidWorks Flow Simulation and adaptive mesh thickening technique (SolidWorks AM), with which we can see that the aerodynamic drag coefficient deviates from the measured value by -9.7%, and the lift coefficient deviates by -19.4%. Drag force, which was in this case calculated with the ANSYS Fluent software, amounts to 16.6 N, and lift force is 19.8 N. Drag force, which was calculated with the CFD software package SolidWorks and adaptive technique, in the final mesh of 6.7 million finite elements, amounts to 14.8 N, and lift force is 12.9 N. The differences in the computational time is crucial. Using the ANSYS Fluent package, the computational part of the analysis took us 43 minutes, simulation performed with a quad-core CPU, and using the SolidWorks software, the time increased to 65 hours.

**Table 1:** Comparison of the results at the inflow velocity of 40 m/s

	Experiment [4]	Fluent RKE-NEQ		SolidWorks	
			$\Delta\%$		$\Delta\%$
$C_D$	0.298	0.297	-0.1	0.269	- 9.7
$C_L$	0.345	0.352	1.9	0.278	- 19.4

## 5.2 Analysis at different velocities

In the second part of the analysis, the results of simulations for different velocities of the air inflow were compared. Using the ANSYS Fluent software, an analysis of simulations with the Realizable k- $\epsilon$  turbulence model with Non-Equilibrium walls treatment (Fluent RKE-NEQ), as well as with Enhanced Wall Treatment (Fluent RKE-EWT), was performed. Using the SolidWorks Flow Simulation software, the case with two meshes, with Coarse (SW-Coarse) and Fine (SW-Fine) mesh without using the adaptive mesh technique were analysed; the Coarse mesh had 2.5 million finite elements, and the Fine mesh 6.5 million elements. Figure 6 displays the results of the calculated drag and lift forces in dependence on the inflow velocity within the range of 10 m/s to 60 m/s, and Figure 7 displays the drag and lift coefficients within the analysis area. At first glance, the results of the different models appear similar for each of the numerical meshes and analysed turbulence models. Furthermore, that the prediction of forces or lift coefficient is significantly higher in the ANSYS Fluent software can be determined.

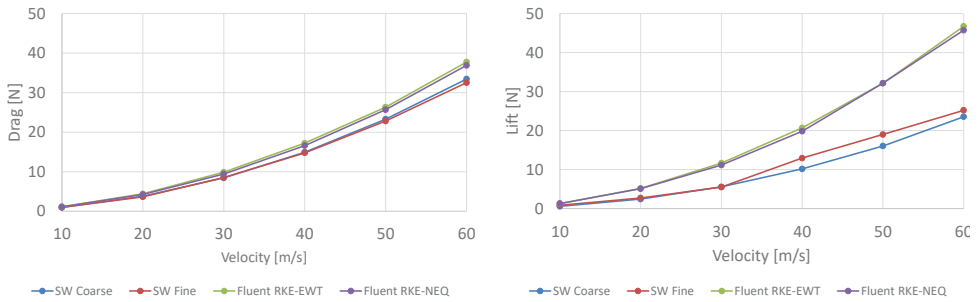


Figure 6: Drag and Lift force versus velocity

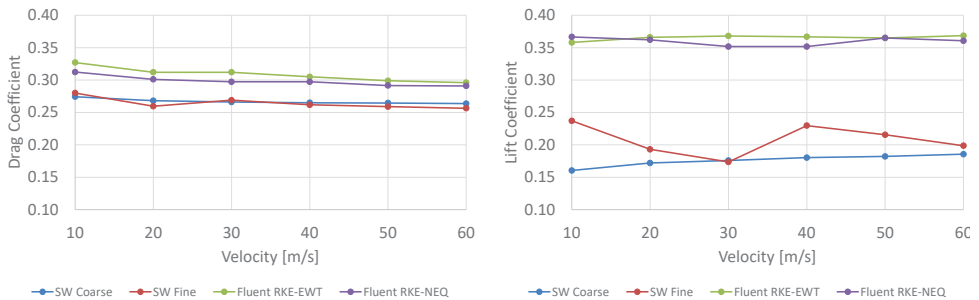
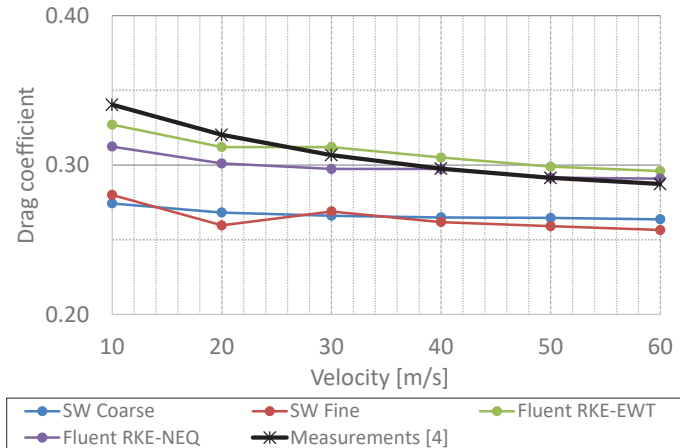


Figure 7: Drag and Lift coefficient versus velocity

Figure 8 shows a comparison between the drag coefficient and published measurements. A significant difference between the measurements and prediction with the SolidWorks Flow Simulation software in the complete analysis field can be determined. In contrast, both turbulence models used in the Fluent software give a very good prediction in the complete analysis area. Nevertheless, in the complete analysis area the same mesh was used, having 2.6 million final volumes. Table 2 displays a summary of the  $y^+$  variable on the walls of the body. In

the analysis area, the value of the variable was between 1 and 163, and on average it was between 16 and 88.



**Figure 8:** Drag coefficient from simulations and measurements

**Table 2:** Variable  $y^+$  on the walls of the body at different velocities using the ANSYS Fluent software

Velocity [m/s]	$y^+_{\min}$	$y^+_{\max}$	$y^+_{\text{ave}}$
10	1	32	16
20	1	61	31
30	2	88	46
40	3.5	114	63
50	5	139	74
60	6	163	88

Figure 9 shows a comparison of the pressure field on the surface of the body and on the plane of symmetry. Despite the fact that at first glance the figures may appear very similar, from the analysis of lift and drag force, we know that there is a significant difference between the integrated value of the pressure distribution. Figure 10 shows a comparison of the velocity contours in both software programmes, namely on the plane of symmetry, as well as on the plane at an altitude of 0.244 m above ground level. In this case, a greater difference in prediction of velocity in front and behind the body can be observed.

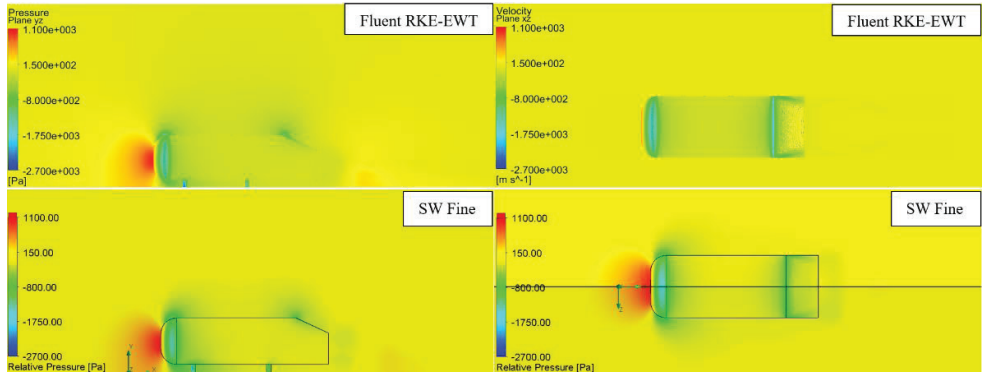


Figure 9: Prediction of pressure distribution at the velocity of 40 m/s

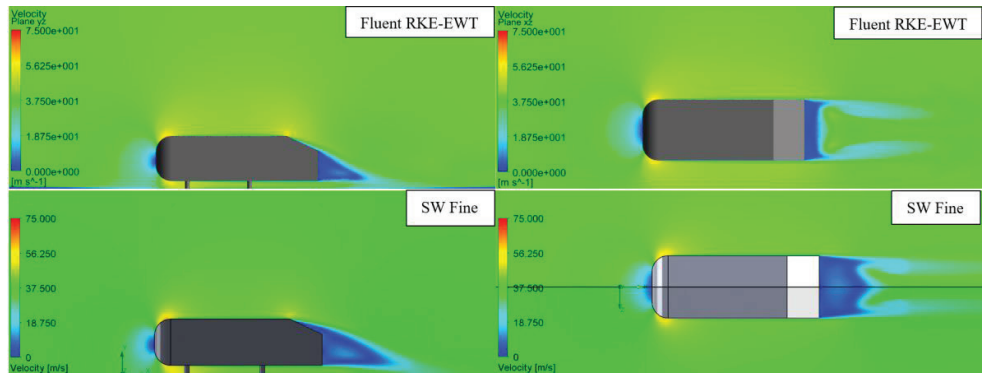


Figure 10: Prediction of velocity distribution at the velocity of 40 m/s

Figure 11 shows a comparison of the turbulent kinetic energy on the plane of symmetry and on the plane at an altitude of 0.244 m above ground level. In this case, it is also obvious that there is a large difference in prediction between the analysed packages.

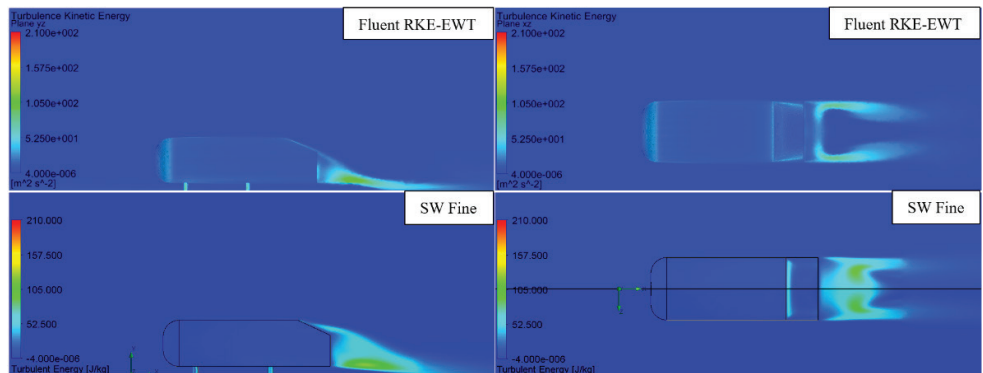


Figure 11: Prediction of turbulence kinetic energy at the velocity of 40 m/s

Table 3 displays the computational times of individual analyses. For the analysis, a computer with an Intel i7 4790 CPU with 16 GB RAM was used. It is apparent from the table that the difference between computational times is significant; using the SolidWorks software, substantially more time for the convergence would be needed.

**Table 3:** Computational times

Computational time [hh]:[mm]				
Fluent RKE-EWT	Fluent RKE-NEQ	SolidWorks Coarse mesh	SolidWorks Fine mesh	SolidWorks adaptive mesh
0:40	0:33	2:40	17:10	65:00

## 6 CONCLUSIONS

The performed comparison analysis of the prediction of numerical analysis with the ANSYS Fluent software package, and the SolidWorks Flow Simulation software package shows a significant difference between the predictions of flow field. With the ANSYS Fluent software, a small deviation from the publicised measured values in a relatively short period is obtained. The SolidWorks Flow Simulation software package is significantly more inaccurate in prediction of results, and needs significantly more time.

The difference between the prediction among different packages can be explored in the technique of meshing as well as in the numerical algorithms themselves. The Cartesian mesh of the SolidWorks Flow Simulation software package did not enable sufficiently precise prediction of the forces on the Ahmed body, despite the extremely long computation time and the adaptive mesh technique. The trend of prediction in the analysed area otherwise follows the correct value, but the difference between the prediction and the measurement is large.

The performed analysis, both from the aspect of results accuracy as well as from that of computational times, shows that purpose-made tools for numerical analysis, such as ANSYS Fluent, are much faster and more accurate than add-ons to 3D modellers, as in the case of SolidWorks Flow Simulation.

## References

- [1] **I. Ščuri, M. Pezdevšek, I. Spaseski, M. Fike and G. Hren**, "Numerical analysis of an axial flow fan: ANSYS vs SolidWorks," *Journal of Energy Technology*, vol. 4, pp. 11-19, 2014
- [2] **I. Spaseski, M. Pezdevšek, I. Ščuri, G. Hren and M. Fike**, "Numerical analysis of lift and pressure coefficient on fan airfoil: ANSYS vs SolidWorks," *Journal of energy technology*, vol. 3, pp. 63-73, 2014
- [3] **S. Ahmed and G. Ramm**, "Some salient features of the time-averaged ground vehicle wake," *SAE Technical Paper 840300*, 1984

- [4] **W. Meile, G. Brenn, A. Reppenhagen, B. Lechner and A. Fuchs**, “Experiments and numerical simulations on the aerodynamics of the Ahmed body,” *CFD Letters*, vol. 1, pp. 32-38, 2010
- [5] **Y. Liu and A. Moser**, “Numerical modeling of airflow over the Ahmed body,” in *Proceeding of the 11th Annual Conference of the CFD Society of Canada*, 2003
- [6] **S. Krajnović and G. Mineli**, “LES investigation of the asymmetry in the wake of a generic vehicle body,” in *4th International conference on Jets, Wakes and Separated Flows, ICJWS2013 IMECE 2013*, 2013
- [7] **C. Hinterberger, M. Garcia-Villalba and W. Rodi**, “Large eddy simulation of flow around the Ahmed body,” in *The Aerodynamics of Heavy Vehicles: Trucks, Buses, and Trains*, Volume 1, 2004
- [8] **M. K. A. B. Salleh**, *Simulation and analysis drag and lift coefficient between sedan and hatchback car*. Bachelor thesis, PAHANG: University Malaysia Pahang, 2009
- [9] **M. Lanfrit**, “Best practice guidelines for handling Automotive External Aerodynamics with FLUENT,” 2005. [Online]. Available: [http://www.southampton.ac.uk/~nwb/lectures/GoodPracticeCFD/Articles/Ext\\_Aero\\_Best\\_Practice\\_Ver1\\_2.pdf](http://www.southampton.ac.uk/~nwb/lectures/GoodPracticeCFD/Articles/Ext_Aero_Best_Practice_Ver1_2.pdf). (25. 10. 2016)

## Nomenclature

$F_D$	Drag force
$F_L$	Lift force
$C_D$	Drag coefficient
$C_L$	Lift coefficient
$Re$	Reynolds number
$p_d$	Dynamic pressure
$A$	Reference area
$k$	Turbulent kinetic energy
$\varepsilon$	Turbulent dissipation
$\omega$	Specific dissipation rate
$\Delta$	Relative difference
$y^+$	Dimensionless wall distance
$v$	Air velocity



# CRITICAL ANALYSIS OF FORMULAE FOR THE CALCULATION OF THE ELECTRICAL PARAMETERS OF HUMID MATERIAL

## KRITIČNA ANALIZA FORMULE ZA IZRAČUN ELEKTRIČNIH PARAMETROV VLAŽNOSTI MATERIALA

Valentyna Zagirnyak<sup>✉</sup>, Borys Nevzlin<sup>1</sup>, Vitaliy Dziuban<sup>1</sup>

**Keywords:** electrical characteristics, material dielectric permittivity, calculation expressions

### **Abstract**

A comparative analysis of conventional calculation expressions for the determination of the electric parameters of humid material has been done. Their disadvantages have been determined, and the errors of their use for calculation of electrical characteristics of a specific material (zinc cake) have been determined. A means of improving the considered calculation expressions has been proposed.

### **Povzetek**

Predstavljena je primerjalna analiza klasičnih računskih izrazov za določitev električnih parametrov vlažnosti materiala. Njihove pomanjkljivosti so nakazale na napake, ki se pojavljajo pri uporabi izračunov električnih karakteristik pri realnem materialu cinkove pogače. Predlagan je način izboljšave obravnavanih računskih izrazov.

---

✉ Corresponding author: Valentyna Zagirnyak, Kremenčuk Mykhailo Ostrohradskiy National University, Department of mechanical engineering, vul. Pershotravneva, 20, 39600, Kremenčuk, Ukraine, Tel.: +38 05366 36219, E-mail address: [mzagirn@kdu.edu.ua](mailto:mzagirn@kdu.edu.ua)

<sup>1</sup> Kremenčuk Mykhailo Ostrohradskiy National University, Department of Electric machines and Apparatus, vul. Pershotravneva, 20, 39600, Kremenčuk, Ukraine

## 1 INTRODUCTION

In many technological processes from coal preparation to grain processing, it is necessary to control material humidity. Essentially, its values determine the energy costs required for preparation of the output product. In its turn, the humidity of the material, irrespective of its chemical composition, as a rule, is determined from expressions taking into account the relation of its values to the values of dielectric permittivity of the corresponding processed material.

At present, several models (calculation expressions for description of the properties) of humid materials are known, [1-15]. They are mainly intended for liquid-water systems, as these systems provide a possibility to find a determined relation between dielectric permittivity (DP) and humidity  $W$ .

Fundamentals of theoretical calculations of DP for liquid-water systems have been established by several authors [4-8, 11-13], but some of them show the relation between DP and humidity implicitly (Tables 1-3, where  $\varepsilon_d$ ,  $\varepsilon_w$  are the dielectric permittivities of the "dry" phase and water, respectively). As the authors are not aware of more recent research in this field, they considered it necessary to perform a critical analysis of the available calculation expressions.

## 2 BASIC MATERIAL OF THE RESEARCH

Let us perform a comparative analysis of the models given in Tables 1–3. Obviously, in Table 1 formula 1.1 can only be applied when the water layer is parallel to impacting electrical (or electromagnetic) field without mixing with the dry phase. Formulae 1.3–1.6 seem to be meant for calculations at low values of humidity as at  $W \rightarrow 1$  they result in a significant error, which is stated in [2].

As to formulae 2.1 and 2.2, it can be noted that they, as well as formula 1.1, seem to be correct for separate layers of water and dry material, but arbitrarily oriented in relation to the electromagnetic field. This is their advantage over formula 1.1. However, in all the other aspects they are rather conditional for the real pattern of location of water in the material.

One of the basic faults of formulae 3.1-3.7 consists in implicit dependences of  $\varepsilon$  on  $W$ . In [2], this fault is eliminated by expansion of formulae 3.1-3.7 in series by degrees  $W$ , which is of the form:

for formulae 3.1, 3.2

$$\begin{aligned} \frac{\varepsilon}{\varepsilon_d} = & 1 + 3W \frac{\varepsilon_w - \varepsilon_d}{\varepsilon_w + 2\varepsilon_d} + 9W^2 \left( \frac{\varepsilon_w - \varepsilon_d}{\varepsilon_w + 2\varepsilon_d} \right)^2 \frac{\varepsilon_w}{\varepsilon_w + 2\varepsilon_d} + \\ & + 27W^3 \left( \frac{\varepsilon_w - \varepsilon_d}{\varepsilon_w + 2\varepsilon_d} \right)^3 \frac{\varepsilon_w(\varepsilon_w - \varepsilon_d)}{(\varepsilon_w + 2\varepsilon_d)^2} + \dots, \end{aligned} \quad (1)$$

for formula 3.3

$$\frac{\varepsilon}{\varepsilon_d} = 1 + 3W \frac{\varepsilon_w - \varepsilon_d}{\varepsilon_w + 2\varepsilon_d} \left[ 1 + W \frac{\varepsilon_w - \varepsilon_d}{\varepsilon_w + 2\varepsilon_d} + W^2 \left( \frac{\varepsilon_w - \varepsilon_d}{\varepsilon_w + 2\varepsilon_d} \right)^2 + \dots \right], \quad (2)$$

**Table 1:** Material dielectric permittivity  $\varepsilon$  explicit direct dependences on humidity  $W$

No.	Author(s) of the formulae	Dependence type and formulae number
1	Silberstein, Newton	$\varepsilon = \varepsilon_d(1 - W) + \varepsilon_w W$ (1.1)
2	Lorenz	$\varepsilon = \frac{\varepsilon_d(\varepsilon_w + 2) + 2W(\varepsilon_w - \varepsilon_d)}{\varepsilon_w + 2 + W(\varepsilon_w - \varepsilon_d)}$ (1.2)
3	Odolevskii (for statistic systems)	$\varepsilon = \frac{(2 - 3W)\varepsilon_d + (3W - 1)\varepsilon_w}{4} + \sqrt{\left[\frac{(2 - 3W)\varepsilon_d + (3W - 1)\varepsilon_w}{4}\right]^2 + \frac{\varepsilon_d \varepsilon_w}{2}}$ (1.3)
4	Odolevskii (for matrix systems)	$\varepsilon = \varepsilon_d \left[ 1 + \frac{3W}{\frac{1 - W}{3} + \frac{\varepsilon_d}{\varepsilon_w - \varepsilon_d}} \right]$ (1.4)
5	Botcher	$\varepsilon = \varepsilon_d \left( 1 + 3W \frac{\varepsilon_w - \varepsilon_d}{\varepsilon_w + 2\varepsilon_d} \right)$ (1.5)
6	Fradkina	$\varepsilon = \varepsilon_d \frac{\sqrt[3]{(1 - W)^2 (\varepsilon_w + 2\varepsilon_d)^2 + 2W(\varepsilon_w - \varepsilon_d)^2}}{\sqrt[3]{1 - W (\varepsilon_w + 2\varepsilon_d)^2 + (\varepsilon_w - \varepsilon_d)^2}}$ (1.6)
7	Reynolds, Hugh	$\varepsilon = \varepsilon_d + \varepsilon_d W (\varepsilon_w - \varepsilon_d) (\varepsilon_d + A(\varepsilon_w - \varepsilon_d))^{-1}$ (1.7)

**Table 2:** Material dielectric permittivity explicit indirect dependences on humidity

No.	Author(s) of the formulae	Dependence type and formulae number
1	Beer	$\sqrt{\varepsilon} = W\sqrt{\varepsilon_w} + (1 - W)\sqrt{\varepsilon_d}$ (2.1)
2	Lichtenecker	$lg \varepsilon = W lg \varepsilon_w + (1 - W) lg \varepsilon_d$ (2.2)
3	Relay (with Runge's correction)	$\frac{\varepsilon}{\varepsilon_d} = 1 - \frac{3W}{W + \frac{2\varepsilon_d + \varepsilon_w}{\varepsilon_d - \varepsilon_w} + 0.523 \frac{\varepsilon_d - \varepsilon_w}{\frac{3}{4}\varepsilon_d + \varepsilon_w} W^{1/3}}$ (2.3)

for formula 3.4

$$\frac{\varepsilon}{\varepsilon_d} = 1 + 3W \frac{\varepsilon_w - \varepsilon_d}{\varepsilon_w + 2\varepsilon_d} \times \left[ 1 + W \frac{\varepsilon_w - \varepsilon_d}{\varepsilon_w + 2\varepsilon_d} \left( 1 + 0.1 \frac{\varepsilon_w - \varepsilon_d}{\varepsilon_w + 2\varepsilon_d} \right) + W^2 \left( \frac{\varepsilon_w - \varepsilon_d}{\varepsilon_w + 2\varepsilon_d} \right)^2 + \left( 1 + 0.2 \frac{\varepsilon_w - \varepsilon_d}{\varepsilon_w + 2\varepsilon_d} \right) \dots \right], \quad (3)$$

for formula 3.5

$$\frac{\varepsilon}{\varepsilon_d} = 1 + 3W \frac{\varepsilon_w - \varepsilon_d}{\varepsilon_w + 2\varepsilon_d} \times \left[ 1 + W \frac{\varepsilon_w - \varepsilon_d}{\varepsilon_w + 2\varepsilon_d} \left( 1 + 0.1 \frac{\varepsilon_w - \varepsilon_d}{\varepsilon_w + 2\varepsilon_d} + 0.36 \frac{\varepsilon_w - \varepsilon_d}{\varepsilon_w + 2\varepsilon_d} \right)^2 + \dots \right], \quad (4)$$

formula 3.6 is expanded as

$$\frac{\varepsilon}{\varepsilon_d} = 1 + 2.19W \left( 1 + \frac{0.37}{\varepsilon_d} \right) \frac{\varepsilon_w - \varepsilon_d}{\varepsilon_w + 2\varepsilon_d} \times \left[ 1 + W \left( 0.5 + 1.1 \left( \frac{\varepsilon_w - \varepsilon_d}{\varepsilon_w + 2\varepsilon_d} \right)^2 \times \frac{1 + \frac{0.74}{\varepsilon_d} - 3 \left( \frac{\varepsilon_d + 0.37}{\varepsilon_w - \varepsilon_d} \right)^2}{1 + \frac{0.37}{\varepsilon_d}} \right) + \dots \right], \quad (5)$$

and formula 3.7

$$\frac{\varepsilon}{\varepsilon_d} = 1 + 3W \frac{\varepsilon_w - \varepsilon_d}{\varepsilon_w + 2\varepsilon_d} \left[ 1 + 2W \frac{\varepsilon_w - \varepsilon_d}{\varepsilon_w + 2\varepsilon_d} \times \frac{2\varepsilon_w + \varepsilon_d}{\varepsilon_w + 2\varepsilon_d} \right]. \quad (6)$$

However, it should be noted that expressions (1)–(6) can be applied to limited values of humidity, because when condition  $W \rightarrow 1$  is met, some series diverge. So, at  $W = 0.9$ ,  $\varepsilon_w = 80$ ,  $\varepsilon_d = 2$  from (1) we obtain

$$\varepsilon = 2 + 5.01 + 11.97 + 27.87 + \dots,$$

and from (3)

$$\varepsilon = 2 + 5.01 + 4.58 + 4.15 + \dots$$

At the same time in formula (6), restricted by three members, under the same conditions, values  $\varepsilon$  approaching  $\varepsilon_b$  are not achieved:  $\varepsilon = 23.18$ .

**Table 3:** Material dielectric permittivity implicit dependences on humidity

No.	Author(s) of the formulae	Dependence type and formulae number
1	Landauer	$W \frac{\varepsilon_w - \varepsilon}{\varepsilon_w + 2\varepsilon_d} + (1 - W) \frac{\varepsilon_d - \varepsilon}{\varepsilon_w + 2\varepsilon_d} = 0 \quad (3.1)$
2	Botcher	$\frac{\varepsilon - \varepsilon_d}{3\varepsilon} = W \frac{\varepsilon_w - \varepsilon}{\varepsilon_w + 2\varepsilon} \quad (3.2)$
3	Clausius-Mossotti, Lorentz, Viner	$\frac{\varepsilon - \varepsilon_d}{\varepsilon + 2\varepsilon_d} = W \frac{\varepsilon_w - \varepsilon_d}{\varepsilon_w + 2\varepsilon_d} \quad (3.3)$
4	Piecara	$\frac{\varepsilon - \varepsilon_d}{\varepsilon + 2\varepsilon_d} = W \frac{\varepsilon_w - \varepsilon_d}{\varepsilon_w + 2\varepsilon_d} + 0.1W^2 \left( \frac{\varepsilon_w - \varepsilon_d}{\varepsilon_w + 2\varepsilon_d} \right)^2 \quad (3.4)$
5	Tareev	$\frac{\varepsilon - \varepsilon_d}{\varepsilon + 2\varepsilon_d} = W \frac{\varepsilon_w - \varepsilon_d}{\varepsilon_w + 2\varepsilon_d} \times \left( 1 + W \left( 0.1 \left( \frac{\varepsilon_w - \varepsilon_d}{\varepsilon_w + 2\varepsilon_d} \right)^2 + 0.038 \left( \frac{\varepsilon_w - \varepsilon_d}{\varepsilon_w + 2\varepsilon_d} \right)^3 \right) \right) \quad (3.5)$
6	Kubo-Nakamuro	$3\varepsilon_w \lg \frac{\varepsilon_w - \varepsilon}{\varepsilon_w - \varepsilon_d} - (\varepsilon_w - 0.74) \lg \frac{\varepsilon + 0.37}{\varepsilon_w + 0.37} = (2.2\varepsilon_w + 0.81) \lg(1 - W) \quad (3.6)$
7	Bruggeman	$\frac{\varepsilon_w - \varepsilon}{\varepsilon_w - \varepsilon_d} \sqrt[3]{\frac{\varepsilon_d}{\varepsilon}} = 1 - W \quad (3.7)$

Some authors [1, 2] mention that many formulae provide much better approximation to experimental results, if the form of the water-material connection dependence on its dielectric permittivity is taken into consideration. Therefore, in the domain of low humidity it is proposed to assume  $\varepsilon_w = 31$  [10], which makes it possible to considerably improve the accuracy of formula 2.1, but the following remains undetermined: condition of applicability of equality  $\varepsilon_w = 80$  and in what correlation (i.e. what part of water has  $\varepsilon_w = 31$ , and what part has  $\varepsilon_w = 80$ ) they are to be taken.

In [16], a model is proposed in the form of evenly distributed particles of the hard phase in an air matrix. As humidity increases, water forces air out and water dielectric permittivity varies from  $\varepsilon_w = 3$  (for the chemically bound one) to  $\varepsilon_w = 80$  (for the free one) in the function of humidity content and according to the law

$$\varepsilon_w = 80 - 77e^{-\alpha_1 u}, \quad (7)$$

where  $\alpha_1$  – constant coefficient, dependent on the type of dry material e.g. for clay of a certain type  $\alpha_1 = 0.44$ .

The analysis of formulae in Tables 1–3 reveals that many of them, especially those from Table 3, practically coincide at low humidities ( $W \approx 0 \div 0.1$ ) and correspond rather well to the experiment. At high humidity values divergence increases both between the formulae and in relation to the experiment. For example, let us compare the results of calculation of  $\varepsilon$  by formulae given in tables 1–3, with the results of experimental determination of zinc concentrate  $\varepsilon$  at the “Electrozinc” plant (Vladikavkaz, Russia). The measurements were carried out in laboratories by Q meters of E9-4 and E9-5a types. Three samples of concentrate (No. 1, 2, 3) different as to the content of zinc and other components by some percent were under control, [17]. The results of measurements and calculations are given in Tables 4–6.

In Tables 4–6, the numbers in brackets in the column corresponding to formula 1.6 are values obtained according to formula 1.6 after its expansion into series according to [12]. Coefficient A in formula 1.7, depending on relation of the ellipsoidal particle axes lengths and its orientation in relation to the field, was assumed equal to 1/3, as zinc concentrate particles are mainly of a spherical shape.

Values  $\varepsilon$  in Tables 4–6 are rounded off to the second figure, as the stated error of experimental determination of  $\varepsilon$  is about 5%. Therefore, it is not necessary to calculate  $\varepsilon$  more accurately and calculation was carried out with three exact figures afterwards rounded off to the second figure.

A comparison of experimental data with the calculated ones demonstrates the following:

1. Results obtained by the groups of formulae 2.3, 3.3, 3.4, 3.5, 3.7 and 1.3, 2.2, 3.1, 3.2, as well as 1.5, 1.6, 1.7, 3.6 at the humidity of 0.04, practically coincide (up to the error of rounding) and are within the range of experimental values close to higher (77 MHz) frequency.
2. At the humidity of 0.08 and, a fortiori, of 0.12, coincidence can be seen in the groups of formulae. However, divergence between the groups is much bigger (up to 0.2÷0.3), and divergence with the experiment grows up to scores of percent even at higher frequencies.
3. Formula 1.2 gives explicitly low results in the completely calculated range of humidity.
4. Value obtained by formulae 1.2, 1.4, 2.1, though considerably different from each other, are mainly within the range of experimental data. Values obtained by formula 1.1 are within the values for the frequency range of units of MHz and less, and by formulae 1.4 and 2.1, within the order of tens of MHz.
5. All the given formulae provide results not depending on frequency, which does not correspond at all to real parameters of all bulk materials analysed by the author (coal and coal charge of Donetsk, Vorkuta and Ekibastuz coal basins; zinc and lead ores; some soils in Luhansk and Moscow regions, as well as in Krasnodar territory; cereals; potassium and other salts). Many authors [18-20] also confirm this conclusion.
6. Almost all the given formulae fail to take into account the shape of bulk particles (apart from 1.7), and package density influence  $\varepsilon_d$  and enters the formulae mainly linearly. At the same time, in practice, according to [14], bulk materials  $\varepsilon$  nonlinear dependence on density takes place.

**Table 4:** Results of measurements and calculations of zinc concentrate  $\varepsilon$  (sample No. 1) depending on humidity  $W$  and frequency  $f$  at  $\varepsilon d=2.2$

No.	$W$ , r.u.	$f$ , MHz	$\varepsilon$ experimental	Values of $\varepsilon$ , calculated by relevant formulae in tables 1–3																			
				1.1	1.2	1.3	1.4	1.5	1.6	1.7	2.1	2.2	2.3	3.1	3.2	3.3	3.4	3.5	3.6	3.7			
1	0.04	2.00	5.3																				
		7.25	4.1																				
		21.0	3.9	2.4	2.5	3.0	2.4	1.2	2.4	3.2	2.5	2.5	2.5	2.5	2.5	2.5	2.5	2.5	2.5	2.5	2.4	2.5	
		77.0	2.9																				
2	0.08	2.00	6.0																				
		7.25	5.3																				
		21.0	4.4	2.4	2.5	2.8	3.8	2.7	1.3	2.7	4.3	2.9	2.7	2.8	2.8	2.8	2.8	2.8	2.8	2.8	2.7	2.8	
		77.0	3.5																				
3	0.12	2.00	11																				
		7.25	8.0																				
		21.0	6.4	2.4	2.5	3.5	4.7	2.9	1.4	2.9	5.7	3.4	3.0	3.2	3.0	3.0	3.0	3.0	3.0	3.0	2.9	3.0	
		77.0	4.5																				



**Table 6:** Results of measurements and calculations of zinc concentrate  $\varepsilon$  (sample No. 3) in the function of humidity  $W$  and frequency  $f$  at  $\sigma d=2.8$

No.	$W$ , r.u.	$f$ , MHz	$\varepsilon$ experimental	Values of $\varepsilon$ , calculated by relevant formulae in tables 1–3																
				1.1	1.2	1.3	1.4	1.5	1.6	1.7	2.1	2.2	2.3	3.1	3.2	3.3	3.4	3.5	3.6	3.7
1	0.04	2.00	5.6																	
		7.25	4.5																	
		21.0	3.9	3.0	3.1	3.7	3.1	1.6 (3.1)	3.1	3.9	3.2	3.1	3.1	3.1	3.1	3.1	3.1	3.1	3.0	3.1
		77.0	3.1																	
2	0.08	2.00	8.8																	
		7.25	7.2																	
		21.0	5.5	3.2	3.5	4.8	3.4	1.8 (3.5)	3.4	5.1	3.7	3.5	3.6	3.6	3.5	3.5	3.5	3.5	3.4	3.5
		77.0	3.9																	
3	0.12	2.00	13																	
		7.25	12																	
		21.0	9.2	3.4	4.1	5.9	3.7	1.8 (3.9)	3.7	6.5	4.2	3.8	4.1	4.1	3.8	3.8	3.8	3.7	3.8	
		77.0	6.3																	

7. Influence of bulk material chemical composition is also expressed via  $\varepsilon_d$ , though at high humidity  $\varepsilon$  dependence on it grows.
8. Dependence of  $\varepsilon$  on humidity is practically linear in all the formulae, though in real bulk materials it is not quite so.

Convergence of calculated and experimental data in the bulk materials electrical theory developed in [3] is better. The authors of this theory managed to obtain root-mean-square deviation of calculated and experimental results of no more than 3–5% for a number of materials (coal charge for coking, wheat, zinc cake, some ordinary coals and soil types and other materials) at the humidity of no more than 10–15%. However, at high humidities, especially for soils, zinc cake and ordinary coals, at the frequencies of units of MHz and less, divergence made scores of percent and, in some cases, hundreds of percent.

Sometimes, experimental values of  $\varepsilon$  exceeded  $\varepsilon$  values for water, which cannot be explained by the error of the experiment. Thus, the theory proposed in [3], does not provide satisfactory explanation either.

### 3 CONCLUSIONS

Based on the above, it can be stated that existing mathematical models of humid bulk materials do not reflect the parameters and characteristics of the real material quite adequately. First, they provide results independent of frequency; they do not take into account the shape of bulk material particles and the nonlinear character of packing density influence. Consequently, they need considerable improvement, including the possibility of changing the approaches.

### References

- [1] Berliner M.A. Humidity measurement. – M: Energiia, 1973. – 400 p. (in Russian)
- [2] Theory and practice of express control of humidity of solid and liquid materials / E.S. Krichevskii, V.K. Benzar, M.V. Venidiktov et al / Edited by E.S. Krichevskii. – M.: Energiia, 1980. – 240 p. (in Russian)
- [3] Dubrov N.S., Krichevskii E.S., Nevzlin B.I. Multi-parameter humidity meters for bulk materials. – M: Mashynostroenie, 1980. – 144 p. (in Russian)
- [4] Lichtenecker K. – Physik Z, 37, 1936, Bd 37, S, 906.
- [5] Büchener A. – Wiss. – Veroffentl. Siemens – Werke, 1939, Bd. 84. S. 18.
- [6] Odelevskii V.M. Calculation of generalized conductivity of heterogeneous systems. – ZhTF, 1951, t.21, issue 6. –P. 667-685. (in Russian)
- [7] Sillars R.W. The properties of a dielectric containing semiconducting particles of various shapes. – J. of the Institution of Electrical Engineers, 1937, vol. 80, № 5, – P. 484.
- [8] Klugman I.Yu. Metrological substantiation of dielectric method of measuring oil humidity: Cand. thesis: 05.11.13 / Kuibyshev Polytechnic Institute – Kuibyshev, 1966. (in Russian)

- [9] Humidity: Measurement and regulation in scientific research and technology. T.4. Principles and methods of measurement of humidity in liquid and solid materials: Trans. from Eng. – Edited by E.S. Krichevskii – L.: Gidrometeoizdat, 1968. (in Russian)
- [10] Eme F. Dielectric measurements. – M.: Chemistry, 1967. –224 p. (in Russian)
- [11] Skanavi G.I. Dielectric physics (weak fields domain). – M.–L.: Gosenergoizdat, 1949. (in Russian)
- [12] Khippel A. Dielectrics and waves. – M.: Foreign literature publishing house, 1960. (in Russian)
- [13] Freidlih G. Theory of dielectrics. – M.: Foreign literature publishing house, 1960. (in Russian)
- [14] Emulsions: Trans. From Eng. – Edited by F. Sherman. – L.: Chemistry, 1972. (in Russian)
- [15] Klugman I.Yu. Factors influencing dielectric permittivity of emulsions of the type B/M // Colloid journal, – 1974. – T. 36, issue 1. – P. 49–53. (in Russian)
- [16] Palmer L.S. On the dielectric constant of the water in wet clay. Proc.Phys. Soc. 1952. B 65.
- [17] Automatic humidity meter for zinc cake / Dubrov N.S., Nevzlin B.I., Kanukov E.Kh. et al. // Non-ferrous metals. – 1976. – No. 8. – P. 33–34. (in Russian)
- [18] Research and development of a model of grain dielectric permittivity taking into account bulk density / Yu.P. Sekanov, V.I. Popov, G.N. Bakhmetieva et al. // Automation and instrumentation of stationary technological processes in plant growing. – M.: Publishing house VASHNIL. – 1989. – T. 122, – P. 61–72. (in Russian)
- [19] Kovekh V.P. Development and research of means of electrical control of arboreal plants state: Author’s abstract of Ph.D. thesis (Eng.); 05.11.13. –Tomsk, 2011. – 19 p. (in Russian)
- [20] Cherepanov P.A. Electric oscillation systems for measurement of agricultural product parameters. – M.: Mashynostroenie, 1987. – 184 p. (in Russian)
- [21] Starkov A.A. Development of devices for drying, saturation and polymerization control during concrete modification by monomer; Author’s abstract of Ph.D. thesis (Eng.); 05.11.13. – Moscow, 2011.–16 p. (in Russian)
- [22] Khuriilava A.K. Development and research of devices for control of construction materials humidity: Author’s abstract of Ph.D. thesis (Eng.); 05.11.13. –Moscow, 2014.– 20 p. (in Russian)
- [23] Podkin Yu.G. Research and development of dielcometric means of operative control for disperse systems with high conductivity. Author’s abstract of Ph.D. thesis (Eng.); 05.11.13.–Moscow, 2008.–21 p. (in Russian)
- [24] Research of electrophysical properties of simulators of bulk material humidity / A.A. Ichitovkin, Yu.G. Podkin, A.S. Zaporozhets et al. // Report at all-union scientific and technical meeting “Humidity measurement of industrial materials and agricultural products”. – Minsk, 1978.–P. 104–105. (in Russian)



# OPTIMIZATION OF MAINTENANCE OF GENSETS USING EXPERT SYSTEMS FOR FAULT DIAGNOSIS

## OPTIMIZACIJA VZDRŽEVANJA GENERATORSKIH ENOT Z UPORABO EKSPERTNEGA SISTEMA ZA DIAGNOSTICIRANJE NAPAK

Željko Hederić<sup>3</sup>, Dejan Barešić<sup>1</sup>, Venco Ćorluka<sup>2</sup>

**Keywords:** Bayes' theorem, fault diagnosis, genset, expert system

### **Abstract**

The usage of expert systems simplifies the determination of the technological condition of the genset, i.e. the fault diagnosis. This results in the optimization of maintenance in technical workshops, which particularly comes into play in military systems in which a great number of technical resources must be maintained. The expert system is based on the "Knowledge Base", obtained by researching and collecting data from professionals who have years of experience in the maintenance of electric generators. The Knowledge Base is made to list the most common faults first; then the hypotheses are associated with a certain probability. The processing of collected information is carried out according to Bayes' method, which is based on the classical probability theory. In order to decide upon a failure happening within the context of certain facts, a calculation of true values is carried out, which will help in developing an ideal diagnostic program during further research.

---

<sup>3</sup> Corresponding author: Dr. Željko Hederić, Associate Professor, J.J. Strossmayer University of Osijek, Faculty of Electrical Engineering, Computer Science and Information Technology, Kneza Trpimira 2B, 31000 Osijek, Croatia, E-mail address: zhed-eric@etfos.hr

<sup>1</sup> University of Zagreb, Croatian Military Academy "Dr. Franjo Tuđman", Zagreb, Croatia, dejan.baresic@suradnik.unizg.hr

<sup>2</sup> J.J. Strossmayer University of Osijek, Faculty of Electrical Engineering, Computer Science and Information Technology, Osijek, Croatia, venco.corluka@etfos.hr

## **Povzetek**

Uporaba ekspertnega sistema za diagnosticiranje napak v generatorskih enotah omogoča poenostavitev določitve stanja posamezne enote in morebitno diagnostiko napak. Rezultati optimizacije vzdrževanja v servisnih delavnicah so izredno pomembni v vojaških sistemih, kjer je potrebno ohranjati nenehno večje število naprav v stanju pripravljenosti. Ekspertni sistem temelji na podatkovni bazi znanj, ki je pridobljena preko zbiranja podatkov iz večjega števila opravljenih preizkusov in izkušenj strokovnjakov z večletnimi izkušnjami s področja diagnostike generatorskih enot. Predlagan ekspertni sistem pri vzdrževanju naprav izvede pregled seznama najpogostejših napak in samodejno izvede diagnostiko z določeno verjetnostjo. Obdelava zbranih podatkov poteka po Bayes-ovi metodi, ki temelji na klasični teoriji verjetnosti. Za določitev možnosti napake na podlagi zbranih dejstev se izvede izračun dejanskih vrednosti, kar omogoča nadgradnjo ekspertnega sistema z nadaljnjimi raziskavami.

## **1 INTRODUCTION**

This paper shows the optimization of the maintenance system of gensets in technical workshops. It is particularly suitable for use in the armed forces, where a great number of mobile gensets is present. They are necessary in case of greater damage and failures in the electrical system, which may occur in the event of natural disasters and war. Therefore, their reliability and availability are vital, in both civilian and the military structures. Due to that, regular maintenance is being carried out, which requires certain financial resources. In addition to such resources, an important issue is also the involvement of specialized staff in the maintenance process. Since a large amount of resources is involved, every simplification of the maintenance procedure, as small as it may be, is essential in saving financial resources and engagement of material, technical and human resources.

In complex systems, such as gensets maintenance processes, the identification of the technical conditions of equipment is the most time consuming, i.e. fault diagnosis.

To formulate a diagnostic algorithm of the equipment states, a systematic study of the behaviour in good working condition and during a failure has been carried out. Collecting data on the failures and their indicators was derived from three key sources:

- technical documentation with the regulations on the quality of the product,
- documents about receiving resources for repair in the past five years, from which the reasons of arrival can be seen, as well as the methods carried out in order to correct the deficiencies,
- by conducting research among the employees with years of experience in the maintenance of gensets.

By consolidating the collected data, a “Knowledge base” has been formed, shown partially in Table 3. The data were processed according to Bayes' theorem, and true values were obtained, which will help in further research to develop an ideal program and special instructions for searching and removing irregularities in the assembled form. This provides a comprehensive understanding of the resources' technical condition before dismantling and achieves the greatest effect in reducing the duration of a repair. In addition to that, the described procedures enable the determination of the scope and complexity of repair and the necessary tools, equipment and spare parts in advance.

## 2 GENSET MAINTENANCE PROCESS

The maintenance process is a complete series of organizational and technical measures exploits to establish the functionality of faulty resources, i.e. to repair corrupted technical features after the resources' usability has passed or after the appearance of random defects. The maintenance process consists of a series of different steps connected with the repair, manufacturing of parts, their control, storage and transport. This process also includes the development of technical documentation, planning, standardization, the supply of materials, spare tools and accessories as well as the refinement and development of technological processes and diagnostic methods, [1].

Due to the large number of technical resources in military systems, methods are continuously elaborated, which contributes to the optimization of maintenance and the work productivity of technical workshops. The important point in optimization is the shortening of repair times, which can be significantly affected by the improvement of technological processes and diagnostic methods. For now, the greatest effect is achieved by an elaborated principle of repairing a set (Figure 1), in which expert systems for failure diagnosis can be applied, which significantly reduces the overall repair time.

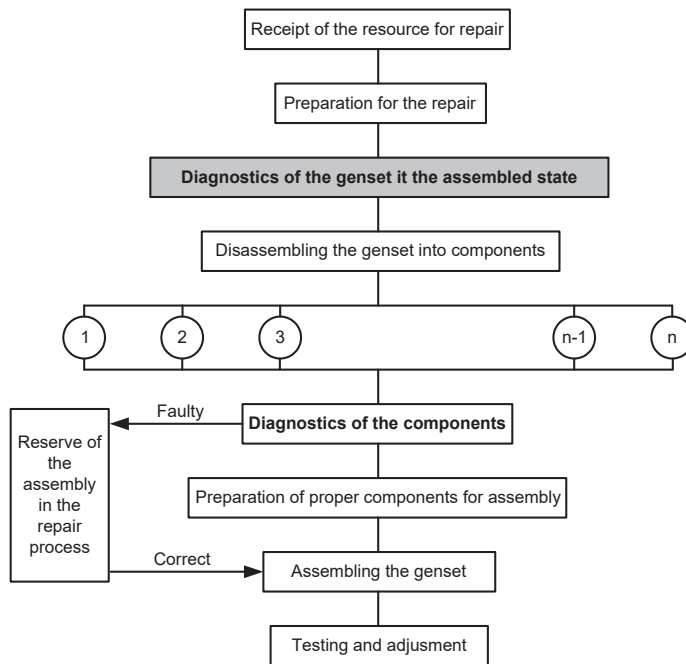


**Figure 1:** Schematic of the technological process on the principle of repairing a set

On receipt of the resource for repair, a protocol for the description of the status is made. Next, the repair and diagnostics are prepared in the assembled state, which represents a complex problem, especially in complex systems such as gensets. Their complexity lies in that they are composed of several technically different subsystems: diesel engine, synchronous generator with excitation, control protection, and connecting and other circuits. This means that for their

diagnostics the criteria which mark the permissible and impermissible states of each mentioned subsystems must be known. Therefore, in order to reduce the time to detect faulty parts, it is necessary to develop an optimal program for fault diagnostic and on the basis of that program to prepare a summary of special instructions for the search for faulty parts.

The use of special instructions for troubleshooting turns random search steps into pre-planned sequences of actions. It is usually easier to locate defective parts when checkpoints are determined, which are used to check for permitted values of technical requirements.

The main tasks of diagnostics in the assembled state are:

- check of the working ability,
- identification of faulty circuits,
- determination of the circuits that need no repair.

The diagnostics in the assembled state is carried out according to the appropriate instructions for each type of genset. The data on irregularities with which the resource is sent and the data on the time and mode of exploitation help to repair diagnose the fault.

The diagnosis is carried out in a specific order, which ensures the completeness of the expected checks and excludes the repetition of certain other checks.

A properly conducted diagnostics provides a comprehensive insight into the state of the resource and enables:

- determination of the scope and complexity of the repair,
- determination of necessary tools, equipment and spare parts,
- determination of employees with certain qualifications (electricians, machinists, mechanics),
- definition of the time required for the repair.

After the diagnostics and detailed insight into the state of the resource, the disassembling continues with the next, so far mostly well elaborated step according to the schematic of the technological process from Figure 1.

### **3 EXPERT SYSTEM FOR DIAGNOSIS OF THE GENSET STATE**

#### **3.1 Knowledge base**

The expert system for fault diagnosis is based on a reliable "Knowledge base", in which the diagnostic features are shown. These data were obtained by studying the standard and the manufacturer's technical documentation, [2, 3, 4], workshop production orders from the previous five years and the implementation of surveys of employees who have years of experience in the maintenance of gensets. The expert system is designed to ensure the rapid determination of genset condition (correct, indication of failure-needed maintenance, fault-needed service). This is an additional tool that connects users and maintenance technicians. Typically, these are two technical levels and are not at the same location neither under the same management. The user (a soldier in the described case) with a basic knowledge of operation during the daily work notes "disturbances" in the work of the genset, which are

categorized in the group of Easily Detectable Failures (EDF). These are linguistic variables with distinctly subjective characters; they are shown in Table 1.

**Table 1:** Example of linguistic variables that describe the group of Easily Detectable Failures with distinctly subjective character

The engine can't start or has difficulties starting
The engine stops a short time after the start
Low engine performance
Low oil pressure
The engine rotational speed drops fast
The engine overheats
The engine throws out thick black smoke
Low generator voltage idling at nominal speed
The generator produces no voltage
The main circuit breaker can't be turned on
Checking the static frequency characteristics - doesn't fulfil the conditions

Based on the detection of disorders from the EDF group, the overseer Expert System focuses further procedures toward maintenance technicians, who represent a higher level of technical knowledge of the genset (a technician in the Repair Institute in the described case). In this process, linguistic variables that describe disorders categorized in group of Hard Detectable Failures (HDF) shown in Table 2 and associated probability of failure from the knowledge base of an expert system have been used.

The importance of resolving the problems of large logistics systems with the use of expert systems that conventional linguistic variables (shown in Tables 1 and Tables 2) convert into digital data should be emphasized. This enables the use of software tools for conducting the control, monitoring and planning of logistics in systems that spatially and hierarchically belong to different sub-systems of management. The general objective is to improve the management of the overall system (military systems in the described case).

**Table 2:** Example of linguistic variables that describe a group of Hard Detectable Failures without subjective character

Damaged fuel supply pipeline
Corroded or loosened connections on the battery
Discharged battery
Fault on the electric starter
Dirty fuel refining system
Dirty air refining system
Faulty injectors
Lack of oil in the motor
Dirty oil refining system
Faulty oil pump
Rotational speed regulator fault
Low engine compression
Loose contact on the voltage regulator
The generator is demagnetized
Faulty mode selector



state of the genset, i.e. the probability of a certain failure which needs to be defined. This probability is called “conditional probability”:  $p(y|x)$ .

$$p(y | x) = \frac{p(x \wedge y)}{p(x)} \tag{3.1}$$

If two events are independent, then:

$$p(x | y) = p(x) \tag{3.2}$$

$$p(y | x) = p(y) \tag{3.3}$$

According to the definition, the revolution, i.e. probability of the event “ $x$ ” under the condition that “ $y$ ” has occurred is:

$$p(x | y) = \frac{p(y \wedge x)}{p(y)} \tag{3.4}$$

$$\text{From(1.3)} \Rightarrow p(y \wedge x) = p(x | y)p(y) \tag{3.5}$$

Because of the commutativity:

$$p(x \wedge y) = p(x | y)p(y) \tag{3.6}$$

Including (1.6) in (1.1), we obtain the simplest form of Bayes' theorem:

$$p(y | x) = \frac{p(x | y)p(y)}{p(x)} \tag{3.7}$$

By expanding the members of the conditional probability, we get Bayes' theorem [5]:

$$p(y | x) = \frac{p(x | y)p(y)}{p(x | y)p(y) + p(x | \sim y)p(\sim y)} \tag{3.8}$$

From Bayes' theorem, we obtain the Bayesian method in production systems:

If “ $x$ ” is true, the conclusion is “ $y$ ” with the probability “ $p$ ”.

With the help of Bayes' theorem, we can conclude the probability of “ $x$ ”.

By interpreting this theorem with the formula (1.7):

- $y$  of the theorem marks an evidence or a fact  $\rightarrow E$
- $x$  of the theorem marks a hypothesis  $\rightarrow H$

$$p(H | E) = \frac{p(E | H)p(H)}{p(E)} \tag{3.9}$$

$$p(H | E) = \frac{p(E | H)p(H)}{p(E | H)p(H) + p(E | \sim H)p(\sim H)} \tag{3.10}$$

In order to decide upon the failure happening with certain facts, a calculation of real values is carried out, as it is elaborated in [6], Chapter 7. For the purposes of determination of correct failure probabilities series of data were collected.

### 3.3 Example case

In order to clarify functioning of the Bayes theorem, the implementation into Expert Systems for fault diagnosis procedures for one common event is presented.

Using genset for the energy supply of sensitive communications equipment requires frequency control of power supply by using built-in indicators' frequencies or portable devices for measuring frequencies. The user (soldier on the ground) noted that the frequency of power supply is outside the permitted areas: EDF → Checking the static frequency characteristics does not fulfil the conditions.

Based on that, the user logs in report into Expert System, which in addition to the description of failure also records the time, date, location of failure, and characteristics of genset (previously classified information in knowledge base).

➤ Case: Checking the static frequency characteristics – does not fulfil the conditions

Expert System based on knowledge base information of probability (Table 3 – shaded row and column) conduct following calculation:

$$p(H_5) = p(\text{dirty fuel refining system}) = 0.1 \qquad p(\overline{H_5}) = 0.9$$

$$p(E | H_5) = (\text{the test of the static frequency characteristics doesn't fulfil the conditions} | \text{dirty fuel refining system}) = 0.8$$

$$p(E | \overline{H_5}) = p(\text{the test of the static frequency characteristics doesn't fulfil the conditions} | \text{not dirty fuel refining system}) = 0.2$$

$$p(E) = p(\text{the test of the static frequency characteristics doesn't fulfil the conditions}) \\ = p(E | H_5) \cdot p(H_5) + p(E | \overline{H_5}) \cdot p(\overline{H_5}) = 0.8 \cdot 0.1 + 0.2 \cdot 0.9 = \underline{0.26}$$

$$p(H_5 | E) = p(\text{dirty fuel refining system} | \text{if it is obvious that the test of the static frequency characteristic doesn't fulfil the conditions}) \\ = \frac{p(E | H_5) \cdot p(H_5)}{p(E)} = \frac{0.8 \cdot 0.1}{0.26} = \underline{\underline{0.30769}}$$

$$\begin{aligned}
 p(H_5 | \bar{E}) &= p(\text{dirty fuel refining system with the fact that it fulfils the} \\
 &\quad \text{static frequency characteristics}) = \frac{p(\bar{E} | H_5) \cdot p(H_5)}{p(\bar{E})} = \frac{(1 - 0.8) \cdot 0.1}{1 - 0.26} \\
 &= \underline{\underline{0.02703}}
 \end{aligned}$$

Comparing  $p(H_5 | \bar{E})$  and  $p(H_5)$  yields the following conclusion:

The fact that the test of the static frequency characteristics does not fulfil the conditions increases the probability of a dirty fuel refining system by approximately 3.1 times.

Table 4 shows the true values for the other cases when the test of the static frequency characteristics does not fulfil the conditions.

This means, by reading Table 4 and comparing the values to those in Table 3, we can, in addition to the abovementioned case, conclude the following:

The fact that the test of the static frequency characteristics does not fulfil the conditions increases the probability:

- of a damaged fuel supply pipeline by 2.5 times,
- of faulty injectors by 1.5 times,
- of a rotational speed regulator fault by 5.2 times,
- of a low engine compression by 3.5 times,
- of a loose contact on the voltage regulator by 1.5 times.

The same procedure must be used to treat the easily observable facts mentioned in Table 1 (and in the first row of Table 3). The given results are, after quick and easy processing by a computer, the foundation for developing an ideal diagnostic programs.

From Table 3 and the presented example case, it is evident that the static calculation checking the frequency characteristics is not associated with all failures listed in Table 2 (and in the left column of Table 3). This is consistent with the fact that, for example, failure of the starter has no effect on the stability of the frequency of the generator power supply.

Some failures have higher and some lower correlation with Easily Detectable Failures, which are listed in Table 1 (first line in Table 3). For example: checking static voltage characteristics is not associated with failure of the starter, whether associated with dirty fuel (because at nominal loads it can lead to instability of diesel engine operation) or the major collapse of genset drive rotational speed. This directly, to a large extent, affects the characteristics of genset frequency, and to a small extent, affects the stability of voltage, as shown in Table 3. The data were confirmed during measurements implemented at genset inspection, [4]. It was determined that a voltage regulator retains a constant voltage to a certain degree of rotational speed collapse, but voltage deviation does noticeably occur at higher and faster changes in rotational speed.

**Table 4:** Calculation of true values for all cases when the test of the static frequency characteristics doesn't fulfil the conditions

Checking the static frequency characteristics - doesn't fulfil the conditions								
	p(H)	p(E   H)	p(E   ~H)	p(~H)	p(E)	p(H   E)	p(H   ~E)	p(H   E)/p(H)
p(H <sub>1</sub> )=	0.200	0.800	0.200	0.800	0.320	0.500	0.059	2.50
p(H <sub>2</sub> )=	0.050			0.950	0.000		0.050	
p(H <sub>3</sub> )=	0.100			0.900	0.000		0.100	
p(H <sub>4</sub> )=	0.010			0.995	0.000		0.005	
p(H <sub>5</sub> )=	0.100	0.800	0.200	0.900	0.260	0.308	0.027	3.10
p(H <sub>6</sub> )=	0.100			0.900	0.000		0.100	
p(H <sub>7</sub> )=	0.050	0.600	0.400	0.950	0.410	0.073	0.034	1.50
p(H <sub>8</sub> )=	0.010			0.990	0.000		0.010	
p(H <sub>9</sub> )=	0.050			0.950	0.000		0.050	
p(H <sub>10</sub> )=	0.010			0.990	0.000		0.010	
p(H <sub>11</sub> )=	0.100	0.990	0.100	0.900	0.189	0.524	0.001	5.20
p(H <sub>12</sub> )=	0.200	0.900	0.100	0.800	0.260	0.692	0.027	3.50
p(H <sub>13</sub> )=	0.010	0.600	0.400	0.990	0.402	0.015	0.007	1.50
p(H <sub>14</sub> )=	0.200			0.800	0.000		0.200	
p(H <sub>15</sub> )=	0.050			0.950	0.000		0.050	

## 4 CONCLUSION

Due to the large number of technical resources in military systems, methods are continuously elaborated, which contributes to the optimization of maintenance. The greatest effect is achieved by the principle of repairing a set, for which the failure diagnosis in the assembled state has a significant role. Therefore, the study of the behaviour of gensets in different states and the development of a Knowledge Base have begun, in which the hypotheses are associated with a certain probability.

With the help of Bayes' theorem true values were calculated, used together with certain facts, to correct the probabilities listed in the Knowledge Base.

The Knowledge Base, containing the elaborated Bayes' theorem and the gathered true values, is the basis for the continuation of the research and development of ideal diagnostic programs and special instructions for diagnosing and troubleshooting.

## References

- [1] **M. Jakopčić:** *Održavanje naoružanja*, Zapovjedništvo Hrvatske kopnene vojske, Zagreb, 2006
- [2] ISO 8528-1 through 8528-6. International Organization for Standardization. Genève
- [3] Upute za rukovanje i održavanje s izvješćem o ispitivanju elektroagregata P-B40.R1 KONČAR-ERS, Rijeka 1995
- [4] Propisi o kvaliteti proizvoda, Elektroagregati izmjenične i jednosmjerne struje, snage do 1 MW, Rade Končar, Rijeka, 1984
- [5] [http://www.zemris.fer.hr/predmeti/is/nastava/Modeliranje\\_neizvjesnosti.pdf](http://www.zemris.fer.hr/predmeti/is/nastava/Modeliranje_neizvjesnosti.pdf) (10. 11. 2015)
- [6] **F. Jović:** *Expert Systems in Process Control*, Chapman & Hall, London, 1992



# INFLUENCE OF SHADING ON I-V CHARACTERISTICS OF THIN FILM PV MODULES

## VPLIV SENČENJA NA I-U KARAKTERISTIKO TANKOPLASTNIH FOTONAPETOSTNIH MODULOV

Matej Žnidarec <sup>✉</sup>, Danijel Topić <sup>1</sup>, Josip Bušić<sup>1</sup>

**Keywords:** Shading, thin-film PV module, amorphous silicon, copper-indium-selenide, I-V characteristic, P-V characteristic, power losses, efficiency

### **Abstract**

Photovoltaic (PV) systems are, numerically, the most widespread type of power plant that harvests renewable energy sources for electricity production. This paper investigates the influence of shading on the electrical characteristics of thin-film PV modules. Two types of thin-film PV modules are used: amorphous silicon and copper-indium-selenide. The electrical parameters of PV modules under various cases of shading are measured, analysed, and presented in tables and charts. A comparison between the electrical characteristics of crystalline silicon and thin-film PV modules under shading showed that thin-film PV modules have more consistent electrical parameters. I-V and P-V characteristics of shape of thin-film PV module are unaffected by shading. The power losses and efficiency of shaded modules are decreasing in linear relation to the increasing shaded area of a PV module.

---

<sup>✉</sup> Corresponding author: Matej Žnidarec MEng, Faculty of Electrical Engineering, Computer Science and Information Technology Osijek, Department of Power Engineering, Kneza Trpimira 2B, 31000 Osijek, Tel.: +385 91 255 1520, E-mail address: [mznidarec@etfos.hr](mailto:mznidarec@etfos.hr)

<sup>1</sup> Faculty of Electrical Engineering, Computer Science and Information Technology Osijek, Department of Power Engineering, Kneza Trpimira 2B, 31000 Osijek

## **Povzetek**

Fotonapetostni sistemi so številčno najbolj razširjena vrsta elektrarn, ki izkorišča obnovljivi vir energije za proizvodnjo električne energije. Članek obravnava vpliv senčenja na električne lastnosti tankoplastnih fotonapetostnih modulov. Uporabljata se dve vrsti tankoplastnih fotonapetostnih modulov, in sicer iz amornega silicija in bakra-indija selenid. V članku se tako merijo in analizirajo električni parametri fotonapetostnih modulov v okviru različnih primerov senčenja. Rezultati so predstavljeni tabelarično in grafično. Primerjava med električnimi lastnostmi silicijevih in tankoplastnih fotonapetostnih modulov v skladu s senčenjem je pokazala, da imajo tankoplastni fotonapetostni moduli bolj dosledne električne parametre. Senčenje ne vpliva na I-U in P-U karakteristike tankoplastnih modulov. Izgube in izplen v primeru senčenja modula se zmanjšuje linearno glede na vse večjo senčenje območja modula.

## **1 INTRODUCTION**

In the 21<sup>st</sup> century, humankind has encountered the problem of global warming because the vast majority of electricity is produced from fossil fuels. According to World Energy Statistics 2016, published by the International Energy Agency, global energy needs can be satisfied by coal only until 2088. Oil reserves will be exhausted by 2060 but, even worse, natural gas reserves will be exhausted by 2053, [1]. Pollution and the climate changes that the usage of fossil fuels are bringing are even more noticeable. During the 1990s, scientists observed rapid changes of global temperature and climate changes, [2]. The response to that was the first attempt to tackle the problems with the Kyoto Protocol, in which world leaders committed their country to reduce gas emissions into the atmosphere, [3]. In 2007, the European Union responded with the 2020 Climate & energy package in which a set of binding legislation ensures that the EU meets its climate and energy targets for the year 2020. Three key targets are a 20% cut in greenhouse emissions from 1990 levels, a 20% improvement in energy efficiency and 20% of EU energy from renewable energy sources i.e. solar energy, wind power, hydropower, geothermal energy and bio-energy, [4]. The framework adopted by EU leaders in October 2014 that builds on the 2020 climate & energy package is the 2030 climate & energy framework with key targets of a 40% cut in greenhouse emission, a 27% improvement in energy efficiency, and 27% of EU energy from renewables, [5]. The ultimate goal for 2050 is a low-carbon economy in which the EU has cut greenhouse gas emissions to 80% below 1990 levels, [6]. Photovoltaic systems (PV) are the most widespread form of harvesting solar energy for electricity production. There are two main types of solar cell technologies used today: crystalline silicon and thin film photovoltaics. Electrical characteristics of solar cells are represented with *I-V* and *P-V* characteristics. The output of a PV module depends directly on input energy from the sun and the temperature of a PV module. If even a small part of irradiated energy is shaded by an object, the output energy of a PV module is significantly reduced, [7].

In [8], the shading influence on the *I-V* characteristic of a mono-crystalline PV module was studied. The results show that power loss depends on the location of the shade on the PV module. If a shade is placed across all six columns of PV cells, horizontally, power decreases by approximately 93%. If a shade is placed across 6 cells in one column, vertically, power decreases by approximately 30%; this does not depend on the number of shaded cells in the same column. Zulu and Kashweka, [9], conducted an experiment of shading of a monocrystalline PV module in three steps, 25%, 50% and 75% of the area. Results showed that in the case of 25% of area shaded, power output was reduced by 75% and efficiency dropped to approximately  $(2.9\% \pm 0.2\%)$ . In the

case of 50% and 75% of the area of module shaded, power output dropped by 90 % and efficiency dropped to approximately  $0.8\% \pm 0.1\%$ . Sun et al., [10], were studying the influence of wire pole shading on electrical properties of six polycrystalline PV modules. The results showed that the power output of modules depends on the number of bypass diodes integrated into the PV module, the size of the shaded area, and the position of the shadow on the PV module surface. Dolara et al., [11], studied the influence of different shading scenarios on monocrystalline and polycrystalline silicon single-cell and whole PV modules. They conducted two shading scenarios for single-cell, right-to-left and bottom-to-top. For a PV module, three shading scenarios were examined: horizontal, vertical and diagonal. A decrease of the power output for every case conducted in this paper does not depend on crystalline technology of which PV modules are made. In [12], [13], [14], [15] and [16], the effects of partial shading on PV arrays characteristics and efficiency are investigated. The main goal of the papers was to propose Maximum Power Point Tracker algorithms, which would extract maximum power from partially shaded PV modules with deformed  $P$ - $V$  characteristics. Bai et al., [17], proposed new physical PV array arrangements to mitigate partial shading effects. Three new physical arrangements are proposed and compared with the performance of existing configurations. While, according to [18], the efficiency and production of thin-film modules is increasing, researchers are neglecting the investigation of this kind of photovoltaics.

This paper investigates influence of shading on electrical characteristics of thin-film PV modules unlike other research studies so far, which only examined crystalline silicon technologies of PV modules.

## 2 METHODOLOGY

### 2.1 Measuring method and instruments

Experiments were conducted on two different technologies of thin film PV modules. The first PV module, named Masdar MPV100-S, uses amorphous silicon technology for electricity production. The second PV module, named Solar Frontier SF150-S, uses copper-indium-selenide (CIS) alloy for electricity production. The technical specifications of Masdar MPV100-S are shown in Table 1, [19, 20].

**Table 1:** Masdar MPV100-S and Solar Frontier SF150-S technical specifications

Parameter	Unit	Masdar MPV100-S	Solar Frontier SF150-S
Nominal peak power ( $P_{MPP}$ )	W	100	150
Nominal voltage ( $V_{MPP}$ )	V	75	81.5
Nominal current ( $I_{MPP}$ )	A	1.34	1.85
Open circuit voltage ( $V_{OC}$ )	V	96	108
Short-circuit current ( $I_{SC}$ )	A	1.56	2.2

Efficiency ( $\eta$ )	%	7	12.2
Temperature coefficient of $P_{MPP}$	%/°C	- 0.2	- 0.31
Temperature coefficient of $V_{OC}$	%/°C	- 0.3	- 0.3
Temperature coefficient of $I_{SC}$	%/°C	0.1	0.01
Dimensions (length x width x thickness)	mm	1300×1100×7	1257×977×35
Weight	kg	29.5	20

The measuring instruments used for the experiments were a Metrix PX110 Powermeter, a Peaktech 3320 DMM, and a Seaward SOLAR Survey 200. The Metrix PX 110 Powermeter is a digital power meter and it is used for measuring the voltage, current and output power of a PV module. The electrical circuit used for measuring the  $I$ - $V$  characteristics of the PV modules is shown in Figure 1.

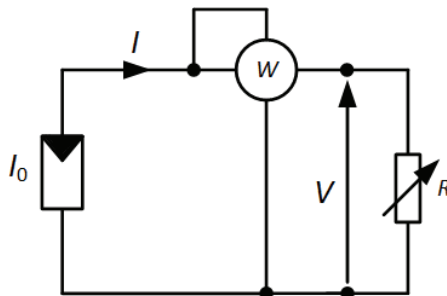


**Figure 1:**  $I$ - $V$  characteristic measuring electrical circuit

A Peaktech 3320 DMM Digital multimeter is used for measuring short-circuit current and open-circuit voltage of the PV modules while a Seaward SOLAR Survey 200 instrument is used for measuring the solar irradiance in  $W/m^2$ .

## 2.2 Shading simulation

The simulated shading profile is divided into 11 steps from the bottom of the module to the top. The first step of the shading profile spreads from the first 10 cm from the bottom edge of the PV module across its whole width. Each next step adds another 10 cm in the height of the module. The final and 11<sup>th</sup> step shades 110 cm of the module from the bottom edge to the top, leaving only small part of unshaded area, which depends on the height of the PV module. Measurement of the  $I$ - $V$  characteristic for each PV module and for every shading case was done according to the electrical schematic shown in Figure 1. The first  $I$ - $V$  characteristic measuring was done for an unshaded area of a PV module. After that, eleven  $I$ - $V$  characteristics for each PV module are measured for each shading case. At the same time as the  $I$ - $V$  characteristic is measured, the

irradiance level was measured. An example of the 1<sup>st</sup>, 2<sup>nd</sup> and 11<sup>th</sup> steps of the shading profile is presented in Figure 2.

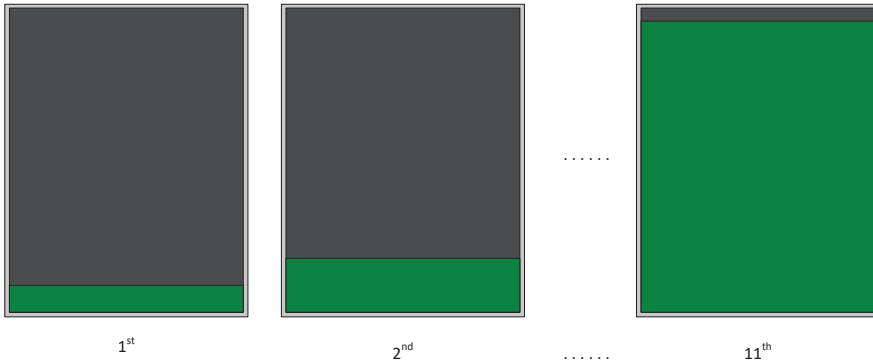


Figure 2: First, second and 11<sup>th</sup> steps of the shading profile

### 3 RESULTS

#### 3.1 Masdar MPV100-S

I-V and P-V characteristics for unshaded and 11 steps of shading profile for a Masdar MPV100-S amorphous silicon PV module are given in Figure 3 and Figure 4. The results reveal that I-V and P-V characteristic's shape does not depend on shading of PV module surface unlike mono- and polycrystalline silicon PV modules. The P-V characteristics given in Figure 4 have only one maximum, regardless of shading case.

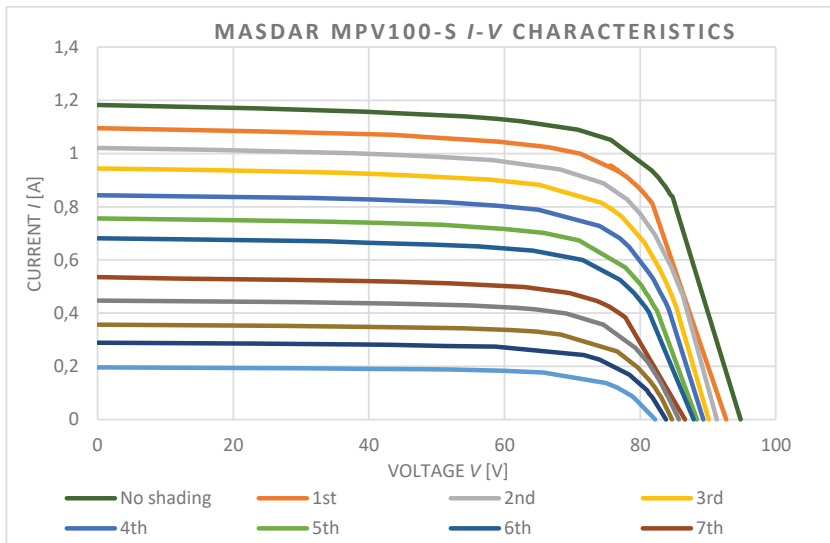
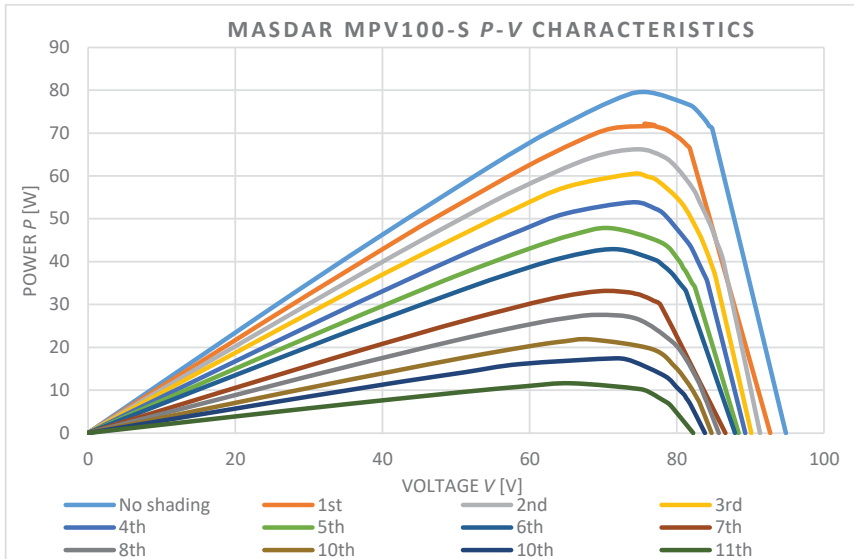


Figure 3: I-V characteristics for unshaded and 11 shading cases of Masdar MPV100-S PV module



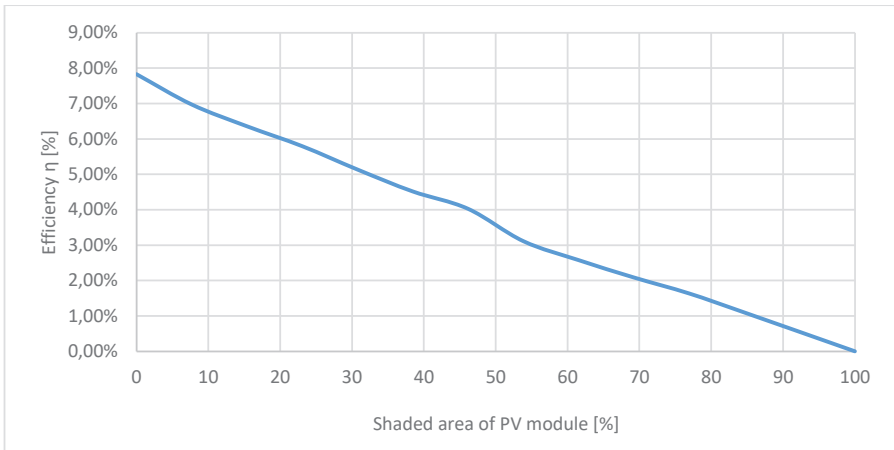
**Figure 4:** P-V characteristics for unshaded and 11 shading cases of Masdar MPV100-S PV module

The processed results for the Masdar MPV100-S PV module for unshaded and 11 cases of shading profile are given in Table 2. The results displayed in Table 2 show that the fill factor  $F$  of the  $I$ - $V$  characteristic does not change in a significant way, regardless of the shading case, which confirms that its shape is not significantly affected.

**Table 2:** Results for Masdar MPV100-S PV module

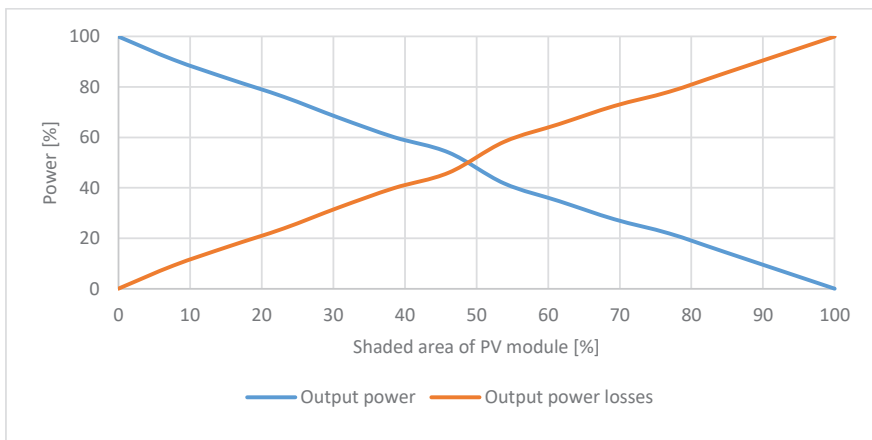
Shading case	Shadow height [cm]	Shaded area of PV module [%]	Output power of shaded PV module $P_n$ [W]	Output power loss $P_L$ [W]	Fill factor $F$ [%]
No shade	0	0	79.5	0	70.95
1 <sup>st</sup>	10	7.69	72.2	7.3	71.06
2 <sup>nd</sup>	20	15.38	66.2	13.3	71.02
3 <sup>rd</sup>	30	23.08	60.5	19.0	71.13
4 <sup>th</sup>	40	30.77	53.9	25.6	71.6
5 <sup>th</sup>	50	38.46	47.8	31.7	71.52
6 <sup>th</sup>	60	46.15	42.9	36.6	71.67
7 <sup>th</sup>	70	53.85	33.2	46.3	71.66
8 <sup>th</sup>	80	61.54	27.6	51.9	72.05
9 <sup>th</sup>	90	69.23	21.9	57.6	72.43
10 <sup>th</sup>	100	76.92	17.4	62.1	71.85
11 <sup>th</sup>	110	84.61	11.6	67.9	72

Figure 5 shows the relation of the Masdar MPV100-S PV module efficiency and shaded area of PV module surface. The curve shows that the efficiency of the PV module is linearly declining with the increase of the shaded area. Small deviations from the linear relation of the sizes are caused by measuring instrument error.



**Figure 5:** Efficiency of Masdar MPV100-S PV module in relation with shaded area

Output power and output power losses of the Masdar MPV100-S PV module in relation with the shaded area is given in Figure 6. Curves presented in the chart are showing that output power and output power losses of the PV module are inversely proportional and in linear relation to the increasing shaded area of a PV module. Small deviations from the linear relation are caused by measuring instrument error.



**Figure 6:** Output power and output power losses of Masdar MPV100-S in relation with shaded area

### 3.2 Solar Frontier SF150-S

Figure 7 and Figure 8 show  $I$ - $V$  and  $P$ - $V$  characteristics for unshaded and 11 steps of the shading profile for the CIS PV module Solar Frontier SF150-S. The results in Figure 7 and Figure 8 show that the shape of  $I$ - $V$  and  $P$ - $V$  characteristics are not influenced by the shading case of the PV module. The  $P$ - $V$  characteristics given in Figure 8 have only one maximum regardless of the shading case

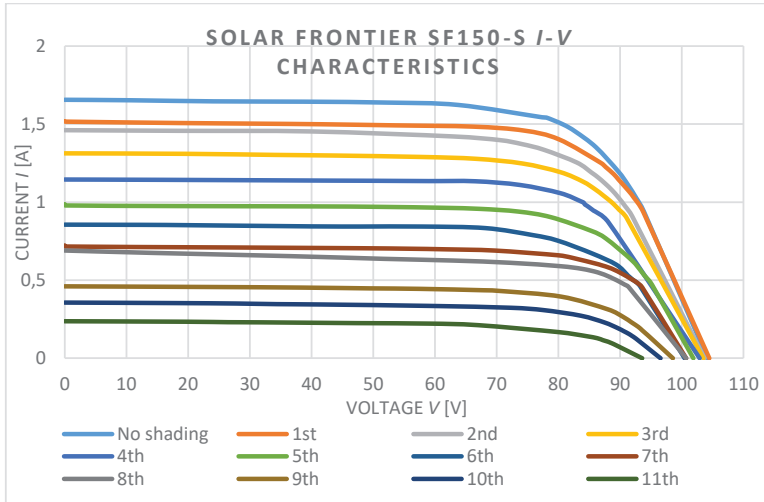


**Figure 7:**  $I$ - $V$  characteristics for unshaded and 11 shading cases of Masdar Solar Frontier SF150-S module

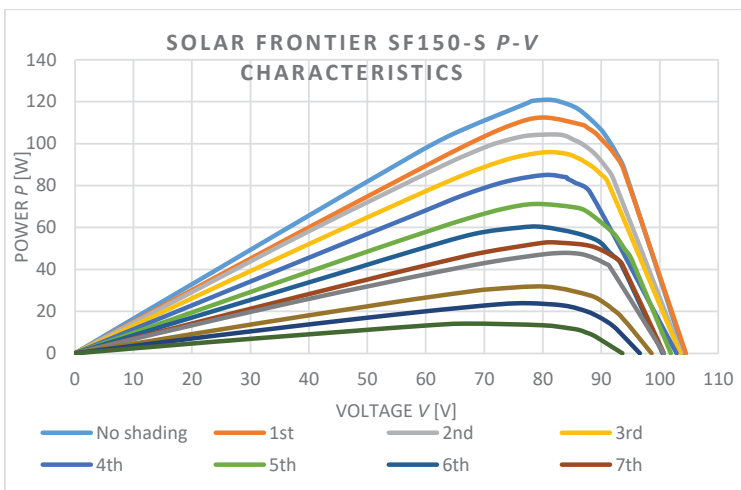


**Figure 8:**  $P$ - $V$  characteristics for unshaded and 11 shading cases of Masdar Solar Frontier SF150-S module

The processed results for Solar Frontier SF150-S PV module for unshaded and 11 cases of shading profile are given in Table 3. As in the former case, fill factor  $F$  is showing that shape of the  $I$ - $V$  characteristic is not significantly affected by the shading.

**Table 3: Results for Solar Frontier SF150-S PV module**

Shading case	Shadow height [cm]	Shaded area of PV module [%]	Output power of shaded PV module $P_n$ [W]	Output power loss $P_l$ [W]	Fill factor $F$ [%]
No shade	0	0	120.9	0	70.11
1 <sup>st</sup>	10	7.96	112.4	8.5	70.76
2 <sup>nd</sup>	20	15.91	104.2	16.7	68.73
3 <sup>rd</sup>	30	23.87	95.9	25.0	70.57
4 <sup>th</sup>	40	31.82	84.9	36.0	72.06
5 <sup>th</sup>	50	39.78	71.2	49.7	70.79
6 <sup>th</sup>	60	47.73	63.0	57.9	73.23
7 <sup>th</sup>	70	55.69	53.0	67.9	72.8
8 <sup>th</sup>	80	63.64	47.9	73.0	69.04
9 <sup>th</sup>	90	71.56	31.9	89.0	70.18
10 <sup>th</sup>	100	79.55	23.9	97.0	69.5
11 <sup>th</sup>	110	87.51	16.0	104.9	72.43

The relation of Solar Frontier SF150-S PV module efficiency and the shaded area of the PV module surface is shown in Figure 9. The curve shows that efficiency of the PV module is declining linearly with the increase of the shaded area. Small deviations from the linear relation of the sizes are caused by measuring instrument error.

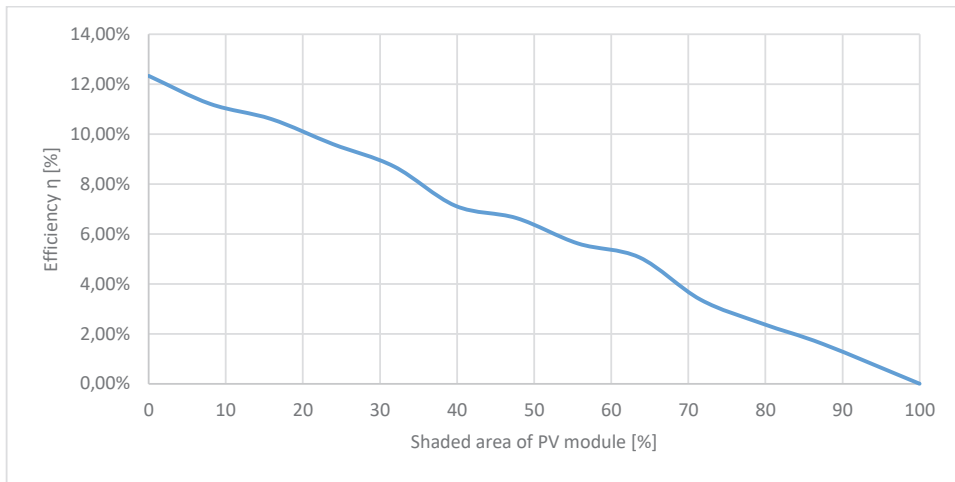


**Figure 9:** Efficiency of Solar Frontier SF150-S module in relation with shaded area

Figure 10 shows output power and output power losses of Solar Frontier SF150-S module in relation with the shaded area. Curves plotted in the chart are showing that output power and output power losses of the PV module are inversely proportional and in linear relation to the increasing shaded area of a PV module. Small deviations from the linear relation are caused by measuring instrument error.

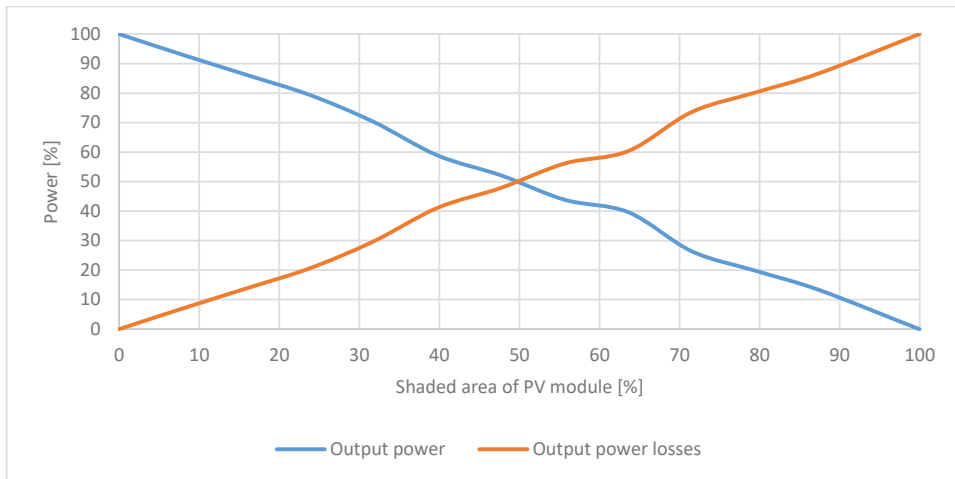


**Figure 10:** Output power and output power losses of Solar Frontier SF150-S in relation with shaded area

## 4 CONCLUSION

This paper studied the influence of shading on electrical characteristics of thin-film PV modules (amorphous silicon and copper-indium-selenide). The influence on the electrical characteristics of the PV modules is measured, analysed and shown in charts and tables. The first difference in the electrical characteristics of crystalline silicon is visible from the shape of the *I-V* and *P-V* curves in a case of shading. The shape of the *I-V* characteristic of thin-film PV modules is unaffected unlike crystalline silicon PV modules, which are drastically deformed. The *P-V* curves of thin-film PV modules have only one maximum, regardless of shading case, unlike crystalline silicon PV modules, which could have a greater number of maximums depending on the number of bypass diodes and position and configuration of solar-cells. Thin-film PV modules can be observed as a single-cell electric generator but crystalline silicon PV modules cannot. They are a set of PV cells connected in series-parallel formation, with a certain number of bypass diodes integrated between them to reduce power losses, depending on the manufacturer. Therefore, if only a single-cell is shaded, its change of electrical characteristics affects the entire PV module. Power losses and efficiency of the thin-film modules are in a linear relation to the shaded area of the PV modules. Since the production price of thin-film photovoltaics is lower than crystalline silicon and the efficiency and production of PV modules is constantly increasing, PV systems based on thin-film photovoltaics are more likely to experience growth in newly installed PV systems. Furthermore, PV systems based on thin-film photovoltaics are more suitable for urban areas in which shading by buildings, utility poles, tree branches, and leaves is a much more common phenomenon than it is in rural areas.

## References

- [1] **International Energy Agency:** *Key World Energy Statistics* [online], 2016. Available: <https://www.iea.org/publications/freepublications/publication/KeyWorld2016.pdf> (12.12.2016)
- [2] **B. C. Black, G. J. Weisel:** *Global Warming*, Greenwood, 2010
- [3] **United Nations:** *Kyoto Protocol to the United Nations Framework Convention on Climate Change* [online], 1998. Available: <https://unfccc.int/resource/docs/convkp/kpeng.pdf> (12.12.2016)
- [4] **European Union:** 2020 climate & energy package [online]. Available: [http://ec.europa.eu/clima/policies/strategies/2020\\_en](http://ec.europa.eu/clima/policies/strategies/2020_en) (12.12.2016)
- [5] **European Union:** 2030 climate & energy framework [online]. Available: [http://ec.europa.eu/clima/policies/strategies/2030\\_en](http://ec.europa.eu/clima/policies/strategies/2030_en) (20.12.2016)
- [6] **European Union:** 2050 low-carbon economy [online]. Available: [http://ec.europa.eu/clima/policies/strategies/2050\\_en](http://ec.europa.eu/clima/policies/strategies/2050_en) (20.12.2016)
- [7] **G. M. Masters:** *Renewable and Efficient Electric Power Systems*, John Wiley & Sons, 2004
- [8] **S. Seme, G. Štumberger:** *Shading effects in the IU characteristic of a mono-crystalline PV module*, XII International PhD Workshop OWD 2010, Wisla, 2010

- [9] **A. Zulu, G. Kashweka:** *The Influence of Artificial Light and Shading on Photovoltaic Solar Panels*, International Journal of Energy Engineering, Vol. 3, Iss. 1, p.p. 15-20, 2013
- [10] **Y. Sun, X. Li, R. Hong, H. Shen:** *Analysis on the Effect of Shading on the Characteristics of Large-scale on-grid PV System in China* [online], Energy and Power Engineering, Vol. 5, p.p. 215-218, 2013. Available: [http://file.scirp.org/pdf/EPE\\_2013101513553018.pdf](http://file.scirp.org/pdf/EPE_2013101513553018.pdf) (13.12.2016)
- [11] **A. Dolara, G. C. Lazaroiu, S. Leva, G. Manzolini:** *Experimental investigation of partial shading scenarios on PV (photovoltaic) modules*, Energy, Vol. 55, p.p. 466-475, 2013
- [12] **A. I. Aldaoudeyeh:** *Photovoltaic-battery scheme to enhance PV array characteristics in partial shading conditions*, IET Renewable Power Generation, Vol. 10, Iss. 1, p.p. 108-115, 2016
- [13] **B. Raja, M. R. Satheesh Kumar, S. Vikash, K. Hariharan:** *Maximum power point tracking in solar panels under partial shading condition using equilibration algorithm*, 2016 International Conference on Communication and Signal Processing (ICCSP), 2016
- [14] **R. Dash, S. C. Swain, P. C. Panda:** *A study on the increasing in the performance of a solar photovoltaic cell during shading condition*, 2016 International Conference on Circuit, Power and Computing Technologies (ICCPCT), 2016
- [15] **M. A. Ghasemi, H. M. Forushani, M. Parniani:** *Partial Shading Detection and Smooth Maximum Power Point Tracking of PV Arrays Under PSC*, IEEE Transactions on Power Electronics, Vol. 31, Iss. 9, p.p. 6281-6292, 2015
- [16] **K. M. Tsang, W. L. Chan:** *Maximum power point tracking for PV systems under partial shading conditions using current sweeping*, Energy Conversion and Management, Vol. 93, p.p. 249-258, 2015
- [17] **N. Belhaouasa, M. S. Ait Cheikhb, P. Agathoklisc, M. R. Oularbid, B. Amrouchea, K. Sedraouie, N. Djilali:** *PV array power output maximization under partial shading using new shifted PV array arrangements*, Solar Energy, Vol. 112, p.p. 41-54, 2015
- [18] **Fraunhofer Institute for Solar Energy Systems:** *Photovoltaics report* [online], 2016. Available: <https://www.ise.fraunhofer.de/de/downloads/pdf-files/aktuelles/photovoltaics-report-in-englischer-sprache.pdf> (20.12.2016)
- [19] **Masdar PV:** *MPV-S - Our a-Si Thin-Film PV Module* [online]. Available: [http://www.secondsol.de/index.php?page=ad\\_showup&ID\\_AD\\_UPLOAD=6630](http://www.secondsol.de/index.php?page=ad_showup&ID_AD_UPLOAD=6630) (15.12.2016)
- [20] **Solar Frontier:** *Product overview SF145-S, SF150-S, SF155-S, SF160-S, SF165-S, SF170-S* [online]. Available: <http://www.solar-frontier.eu/fileadmin/content/downloads/modules/en/20141030/product-overview-s-series-english.pdf> (15.12.2016)

# GROUNDING SYSTEM TESTING USING A LOW-VOLTAGE U-I METHOD – SOME PRACTICAL ISSUES

## TESTIRANJE OZEMLJITVE Z UPORABO NIZKONAPETOSTNE U-I METODE – PRAKTIČNA VPRAŠANJA

Ivan Tolić<sup>✉</sup>, Vedran Angebrandt<sup>1</sup>, Ivana Hartmann Tolić<sup>2</sup>

**Keywords:** grounding, low voltage method, maintenance, legislative

### **Abstract**

This paper deals with practical details of grounding system testing procedures in high-voltage substations. First, the low voltage U-I test method and the relevant legislation are presented. Next, the problems with practical implementation of the method and interpretation of the legislative are extensively described. At the end, the critical overview of the presented method considering possible influence on the decision-making process is given.

### **Povzetek**

Članek predstavlja praktične podrobnosti sistema testiranja ozemljitve v visokonapetostnih podpostajah. Na začetku je predstavljena nizkonapetostna U-I testna metoda in pripadajoča zakonodaja. V nadaljevanju je podrobno opisana problematika praktične implementacije metode in interpretacije zakonodaje. V zaključku je podan kritičen pregled predstavljene metode z ozirom na možne vplive na postopek sprejemanja končne odločitve.

✉ Corresponding author: Ivan Tolić, Croatian Transmission System Operator Ltd., Measurement and Metering, Kupaska 4, 10000 Zagreb, Tel.: +385 91 217 7128, E-mail address: [Ivan.Tolic@hops.hr](mailto:Ivan.Tolic@hops.hr)

<sup>1</sup> Croatian Transmission System Operator Ltd., Measurement and Metering, Kupaska 4, 10000 Zagreb

<sup>2</sup> Faculty of Electrical Engineering, Computer Science and Information Technology Osijek, Department of Software Engineering, Kneza Trpimira 2B, HR-31000 Osijek

# 1 INTRODUCTION

The main challenge in modern power systems is to supply sufficient electricity at any place and at any time needed. Behind this lies a complex power system that has to fulfil that task. In parallel with increasing electricity demand, the power system is developed and over time requires an increasing amount of knowledge and effort spent in proper development and maintenance.

The grounding system is one of the main components of the electric power system and is essential for its safe and reliable operation. Therefore, particular attention is given to its maintenance. Legislation (regulations and recommendations) are the basic guidelines for which maintenance is performed properly, and it is necessary to have correct and complete regulations for maintenance.

The paper presents some implementation problems of the ordinance on technical requirements for power system substations with nominal AC voltage above 1 kV on measuring voltage conditions in high voltage substations. Maintaining the grounding is especially indicated as an integral part of substation maintenance process, and a critical review of the measurement results obtained in accordance with these regulations is presented.

## 2 GROUNDING IN HIGH-VOLTAGE SUBSTATIONS

### 2.1 Grounding definitions

Grounding is defined as the totality of all equipment and measures for grounding, while “to ground” means to connect electrically conductive parts with the earth through the grounding system, [1], which is an important part of every power system. Three basic types of grounding are defined:

- Protective grounding

Grounding conductive parts that are not active parts, in order to protect people from electrical shock. Protective grounding means that electrically connected conductive metal parts are connected to the ground. It needs to ensure carrying away of unwanted currents (as a result of a malfunction in the electrical system, the failure on the consumer side, static charge, signal interference, switching surge, etc.), with the shortest and fastest route to the ground.

- Operational grounding

The grounding point of the active circuit, which is necessary for the proper operation of equipment and facilities. This implies a transformer or generator star-point grounding, directly or indirectly in order to achieve the desired network configuration.

- Lightning grounding

Grounding for carrying away lightning current into the ground requires a safe way for removing unwanted charges and currents that result from atmospheric discharges (lightning).

In this paper, only the high voltage (HV) electrical power stations are considered, so it is important to emphasize that different types of grounding in these facilities are not used separately but for all purposes is used one combined, grounding system.

## 2.2 The design of grounding in HV substations

Grounding systems are metal parts buried into the ground in order to establish a galvanic connection of the grounded part to the ground, [2]. Grounding is part of the overall grounding system that is directly deposited into the soil, [3]. The basic requirement for grounding is that its cross-section is big enough so it could take away high fault current in a short time. The material of which grounding is built must have good electrical conductivity and must not corrode under the conditions that are present in the soil. The most commonly used materials are copper and galvanized iron strips, primarily because of their good conductivity and corrosion resistance. Aluminium is sometimes used for parts of grounding systems that are above ground, but the regulations in most states prohibit such material for grounding because of the possibility of accelerated corrosion. The oxide layer formed as a corrosion product is not conductive, so it can reduce the effectiveness of the grounding. Grounding can be made in various shapes such as vertical rods, plates or horizontal mesh grounding. In HV stations, mesh grounding is used that is of the same order of magnitude as power station where it is placed, [4].

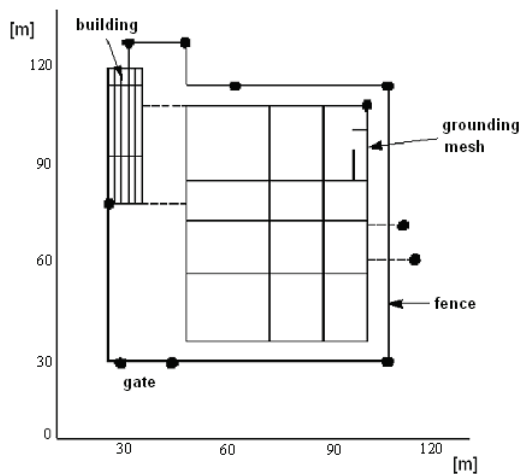


**Figure 1:** The principal scheme of the grounding mesh in relation to the substation fence

Figure 1 shows the position of the grounding mesh in relation to the substation fence. In order to present the order of magnitude of the substation ( $100 \times 100$  m and more), the grounding scheme was put into a coordinate system with pointed axes in meters. Particular attention needs to be paid to the choice of materials of which the grounding will be made. Because of the above-mentioned properties, the most common choice for building the grounding mesh is galvanized iron bar, while copper cable has been used in recent years. When designing the grounding, certain requirements should be met. The designer must project the grounding to meet all the requirements in an optimal way (the technical achievement of objectives at minimum cost).

Therefore, to achieve optimal costs it must be buried at the optimal depth, which means the following:

- a) It must be buried deep enough to avoid the influence of atmospheric conditions on the ground surface. This provides an optimum conductivity of the surrounding ground during the whole year. If it would not be fulfilled it could happen that the soil freezes as a result

of cold temperatures, reducing its conductivity and thus directly increasing the propagation resistance of grounding. The same effect occurs when reducing or increasing the humidity of the soil.

- b) It must be buried deep enough to achieve the optimum potential of the soil over the grounding. By increasing the depth of burial, the potential of the soil surface above the grounding decreases. Metal parts in the substation are connected to the grounding, which means that they achieve its voltage potential. After increasing the depth of burial, the soil surface potential decreases and the potential difference between ground and the metal masses is increasing. This increases the touch potential. The latter problem is particularly emphasized in substation fences where humans being are directly exposed to the touch potential. This is solved by forming potential around a fence.

In order to satisfy all these demands, it is experientially concluded that the optimum depth of grounding burial is at about 0.8 m.

### **2.3 Important parameters for the assessment of grounding system validity**

The consequences of increasing the soil potential are touch and step potentials, and the potentials transferred through a cable bushing towards the next substations, [5].

Step potential is a part of the grounding potential, due to the ground fault, that can be bridged by a step of 1-m length, assuming that current is flowing through the human body from one foot to another. When a person stays with both feet on different potentials, the difference of potential is the step potential where current flows from one foot to another. This voltage depends on the gradient of the potential along the distance from the grounding. If the potential gradient is higher, the person will bridge a larger potential difference.

Touch potential is a part of the grounding potential, due to the ground fault, which can be bridged with the assumption that the current is flowing through the human body from hands to feet (horizontal distance from the accessible portion is 1 m). In that case, the human is at such a distance from that the grounded metal surfaces can be reached; the two points that are at different potentials are bridged. One is a grounded metal mass that is at the potential of grounding, while the other is soil that is at a lower potential. This potential difference is the touch potential. It depends on the potential gradient in a way that the decrease of potential with distance from the grounding touch potential increases. However, when moving away from the grounding, it is no longer meaningful to talk about the touch potential because then the metal surfaces are out of reach. If, after installing the main (mesh) grounding, sufficiently low touch potential is not achieved (according to the regulations), additional grounding for forming the potential is needed as described above.

In order to keep the touch voltage and the step voltage in permitted levels, the suitable arrangement of grounding systems and potential forming is used, [6].

Transferring the potential from substations through the buried metal installations in remote areas remains a problem that arises in the case of earth faults. Due to the flow of current from the grounding network to the ground, the potential of the ground is rising. Equipotential lines (lines of the same potential) follow a form of grounding in its vicinity, while with increasing distance tend to assume the shape of a sphere. If other metal objects are present near the

grounding network or attached to it, there is a distortion of equipotential lines. This means that the potential near a metal object is no longer declining in the funnel shape of the potential around the grounding system, but decreases more slowly or keeps a constant value. One such example is shown in Figure 2.

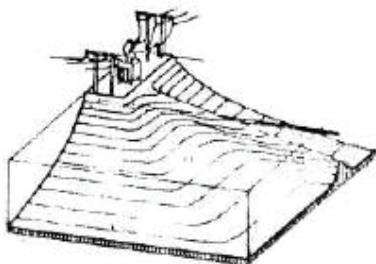


**Figure 2:** Potential funnel in the direction of cable exit

The figure clearly shows the funnel-shaped potentials around the substation and equipotential lines. However, around the cable bushings comes the distortion of equipotential lines in terms of the slower decline of potential which can lead to transmission of this potential in remote areas and in adjacent substations. That would not be expected if the potential would be falling into the funnel shape around the entire substation.

The dangerous consequences of transferring the potentials are:

- a) the risk of touch potential for the people who come into contact with the transferred potential,
- b) thermal overload of metal cable shield due to increased currents,
- c) electrical insulation overexertion.

## 2.4 Testing method

Reliable and correct operation and safety of personnel and equipment are the basic requirements of the existing technical regulations on substations in the case of earth faults. Theoretical considerations and calculations are not enough to predict and describe all phenomena on grounding in fault conditions. Therefore, after the construction of the substation, as well as periodically during its operation, the measurements on grounding are performed. After construction, the measurements are performed to examine the validity of the project and performance of grounding in order to physically verify the designed parameters. During the exploitation, measurements are performed periodically to determine the changes in grounding. Measurement of voltage conditions is performed using a low-voltage (U-I) method, which involves measuring the potential of the grounding and the transferred potential, equipotential lines recording and measurement of touch and step potentials. The principle of the low-voltage measurement method lies in the fact that the application of AC voltage, whose frequency is approximately equal to the frequency of the system, between the grounding system and distant grounding, results in the current  $I$ . Hence, the measurable potential occurs on the grounding. The measured values of the potential and touch and step voltages are then proportionally

recalculated to the maximum current that can flow through the grounding of the object due to the primary single-pole short circuit.

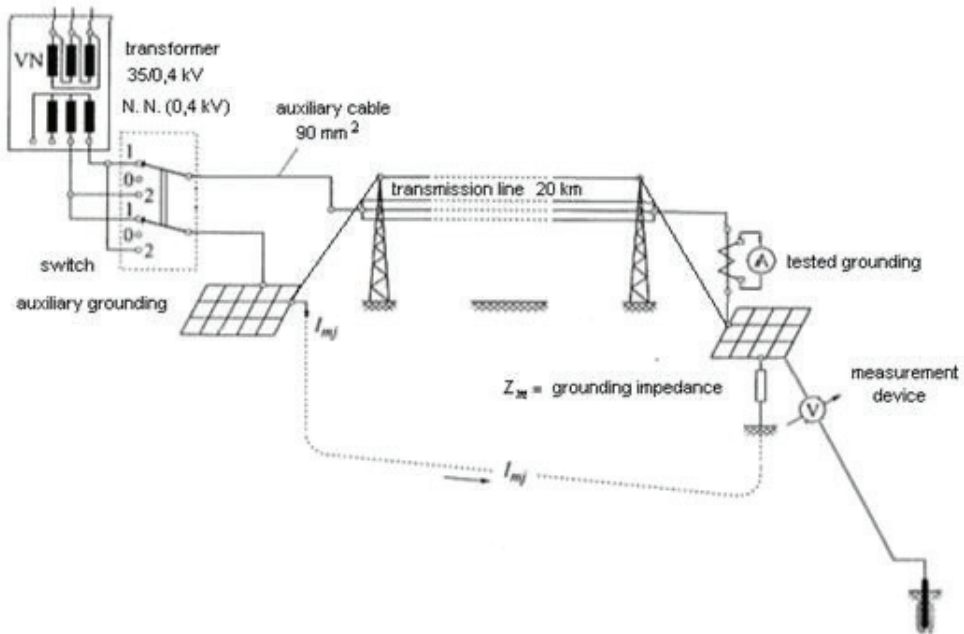


**Figure 1:** The principal scheme of grounding measurements using U-I method

The results obtained and recalculated to the highest single-pole short-circuit current represent voltage conditions on grounding that would appear in case of single-pole earth faults in the substation or on the transmission line and serve as a basis for further decisions on the condition of the substation and possible corrective action to the grounding, [7].

### 3 THE APPLICATION OF EXISTING LEGISLATION ON GROUNDING SYSTEM MAINTENANCE IN HV STATIONS

In November 2010, "Ordinance on technical requirements for power system substations with nominal AC voltage above 1 kV" (NN 105/2010)[8] became valid, replacing "Regulations on technical standards for power system substations with nominal voltage above 1000 V" (Official Gazette of SFRY, no. 4 / 74 and 13/78, article 53 of the Law on Standardization -"Official Gazette no. 55/96 and Article 39, paragraph 1 of the Law on Technical Requirements for Products and Conformity Assessment - Official Gazette, no. 20 / 10) [9]. In accordance with amendments to the legislation, the method of measurement is adjusted. The new regulation regarding the voltage conditions on the grounding refers to International standard EN 50522 accepted as Croatian Standard HRN EN 50522:2010, [1]. With this act, the recommendations contained in the Croatian standard become obligatory.

Furthermore, some of the details and problems of application of the legislation on maintenance of grounding are described, as well as suggestions for improving future versions of the legislation.

### **3.1 Details of applying legislation in terms of maintaining the grounding in HV substations**

Measurements of voltage conditions on grounding in high-voltage substations are performed, aiming to define the statement about the acceptability of voltage conditions at the moment of the ground fault, i.e. about the safety of people and property at the substation and its vicinity. In the case of death of people and property damage, the question of responsibility could be stated. Furthermore, the question of to what level of detail the legislation defines the procedure for testing the grounding and determining the key parameters for safety raises. Therefore, this section deals with the question of how much freedom the legislation leaves to measurement procedure and what consequences it can have on the final statement about the acceptability of voltage conditions.

The valid standard for grounding in HV substations recommends the U-I method, following simple guidelines; however, that is all written based on a principled understanding of the method. Details of the implementation of a measurement procedure are the result of logical reasoning and assumptions of the measurer, so in the case of an investigation of the possible occurrence of hazards at the station or its vicinity, despite the acceptable measurement results, measurements could become unreliable.

Furthermore, the more details that are not completely regulated by law are considered. Finally, possible consequences of incorrect assumptions on final decision considering acceptability of voltage conditions are assessed.

#### **3.1.1 Time limits for testing grounding**

Testing of the grounding is performed after the construction of substations within which is the grounding as well as periodically during normal operation. After applying the “new” regulations, time limits for testing voltage conditions at the grounding was reduced from 5 to 4 years (Article 71, paragraph 1). However, a misunderstanding arises, when reading Article 67 Paragraph 4, which states the following, [8]:

*(4) Maintenance of substations that has been performed or is performing in accordance with regulations applicable earlier must be such that, during the substation lifetime, the technical characteristics of the substation are preserved and that they meet the requirements of the building design regulations and are in accordance with which the substation is made.*

Does this mean that the new regulations do not apply to existing substations rather than the maintenance of such facilities are carried out in accordance with the old regulations?

### 3.1.2 The impact of weather conditions

Weather conditions can have a significant impact on the measurement results, especially on touch and step potentials. It is clear that changes in humidity and specific soil resistance change test results, however, the question is how great this change is [10, 11]. If the change is small compared to the measurement results, the measurement could be performed under any weather conditions (dry soil, moist soil, etc.). However, what if this change is not negligible? The law does not define the impact of weather conditions on the measurement results and therefore does not determine or recommend the conditions under which the measurement must be or should be performed.

### 3.1.3 The influence of the measurement equipment

The impact of measurement equipment is also not negligible. The law does not prescribe which way current is to be injected into the electrical measuring circuit. This is done using a substation distribution transformer that connects via cable to a transmission line. The test current is 50-100 A. For this current cable with copper conductor cross section  $16 \text{ mm}^2$  would be sufficient. With long-term measurement cable heating could be caused, so test current would be reduced. This would result in different test currents during a single measurement. That would hinder the process of recalculation of measured results on the actual short-circuits. It is obvious that it is necessary here to use a larger cable cross-section (e.g.  $90 \text{ mm}^2$ ). The question is how much changing the test current is allowed during the measurement. The law does not prescribe anything about that so the question remains open.

### 3.1.4 The amount of test current and duration of measurement

In relation to the preceding paragraph, the question is raised about the amount of test current and duration of the measurements. Croatian standards state that test current shall be such that the measured values (potential of grounding, touch, and step potentials) at the test current must be greater than the disturbance voltage. However, how much greater is not stated. It is stated only that it is generally achieved with a test current of 50 A. The question is how to achieve that current. Measures to achieve a sufficient amount of test current are not defined in the regulations. It is not advisable to use excessive current that can dry out the soil over long-term measurements. The question is how long the optimal duration of the measurements is and what the optimal test current is.

### 3.1.5 Location of test current injection in tested grounding

When closing the current measuring circuit, it is necessary to specify the location of the injection of test current in tested grounding. The question is on which location is it allowed to do so. The law does not prescribe anything about it, so it can be concluded that it is possible anywhere, e.g. on a substation fence. The most commonly chosen location is where a short circuit can realistically occur. Once the connection to the arbitrarily chosen point is set, the question arises of whether at that point good connection with a grounding in the soil is made. If not, the results of measurements could be completely wrong. The logical solution is to inject current in many places, but that would extend the duration of the measurements. Whether to measure in several locations and how the law does not specify, so the question remains open.

### **3.1.6 Measuring the potential of the grounding**

The grounding potential is measured between the grounding and distance soil. The question that arises here is when an area can be called distant soil and how far is that and how to determine it. An order of magnitude of distance and how it is determined, however, have no legal basis but is determined based on years of experience. The material from which the probe is made is also not determined. Chemical reactions of the soil and the probe could lead to the creation of additional potential, which would undermine the results of measured potential.

### **3.1.7 Reduction factor of protection rope**

For the calculation of current through the grounding, which is relevant for further calculation, a reduction factor of the protection rope is considered. The question is how to determine the exact reduction factor. The Croatian standard recommends a method for calculating on the basis of self-impedance of phase conductor and protection rope. The self-impedance of the phase line depends mostly on the average distance between the phase conductors and protection rope from which it is obvious that the calculation of the reduction factors will not give exact but only approximate values. The procedure for measuring the reduction factors are not determined or recommended. Therefore, the influence of protective rope is taken into account only approximately and the exact impact, because of ignorance of the exact reduction factors, remains unclear.

### **3.1.8 Drawing a grid for recording equipotential lines**

When generating ancillary measure documentation for the purpose of recording the equipotential lines, it is necessary to make a grid over the area around the substation in order to locate the points for measuring the potential. The question is how much that grid must be dense or how many measuring points should be placed on the substation surface. Therefore, the optimal number of measuring points and the way they are distributed throughout the substation are not determined or recommended, so it remains the arbitrary decision of the measurer. Is it even necessary to measure the potential and record equipotential lines and whether there would be other ways to determine dangerous touch and step potentials? The legislation says nothing on this, so these questions remain open.

### **3.1.9 Determination of measurement points to measure touch and step voltage**

After determining equipotential lines, it is necessary to locate points of abrupt change in potential and to identify those points as possible sites of dangerous touch and step potentials. The question that arises is at which point sudden changes in potential is enough so that they can represent a possibly dangerous place. Furthermore, it is unclear whether it is permissible to measure touch and step potentials in the places of the maximum potential gradient, and if they are within acceptable limits to conclude that touch and step potentials at other locations in the substations and outside it are within the allowable limits. The question is what precision is needed in the gradient analysis. The precision of gradient analysis increases proportionally to the number of

points where the potential is measured. The Croatian standard does not state anything about choosing locations for performing measurements of touch and step potentials.

### **3.1.10 Transferring the potential to the surrounding objects**

As a part of high voltage grounding testing, the transferred potential in the surrounding objects is also measured. Regulations applicable to low-voltage systems prescribe the dependence curve of touch potential in low voltage systems on the total switch-off time in case there is a risk of the transferred potential, but does not define the allowed amount of grounding potential in that substation. Croatian standards do not prescribe the exact values of permitted transferred potential. In many publications, the allowed amount of the transferred potential in the buildings are up to 50 V; however, there is no firm foundation for that amount.

### **3.1.11 Interpretation of Regulations**

The terms of the ordinance are left to the subjective interpretation of the reader, and it is, therefore, necessary, in order to use it correctly, to appoint a person or institution to be responsible for their interpretation.

## **4 CONCLUSION**

After a review of the details of the measurements procedure, the conclusion is that the measurer has great freedom and the ability to influence the results. A number of these influences and subjective decisions can significantly alter the results of measurements. Thus, the question is what if one would have to ensure the reproducibility of the measurement results, i.e. if the significant precision has to be achieved (closeness of results of repeated measurements) but with changes of influential factors (measurer, measuring equipment, weather, time interval). Comparing the two different measurers and their measurement procedures, all the details of the measurement procedure that are left to subjective decision-making (not prescribed by legislation) could be different. It is highly possible that the results of measurements are different. Hence, the question is which measurement procedure is correct and whether the results of these measurements are credible at all.

The following point becomes very serious because the results are the basis for deciding on the admissibility of voltage conditions under which commissioning of substations will be granted. In the case of misinterpretation of test results and endangering people and property, all the freedom that the legislation has allowed to the measurer becomes a disadvantage because a subjective decision, i.e. one without legal basis, cannot provide a firm foundation to confirm the credibility of measurement results.

It is necessary to direct a significant amount of knowledge and resources in scientific and technical research in this area in order to resolve at least some of the above-mentioned problems. Implementation of these solutions in the legislation is essential to achieve significant progress in terms of the reliability of power systems and, most importantly, in terms of safety of people and property.

## References

- [1] **'Earthing of power installations exceeding 1 kV a.c. (EN 50522:2010)'**, 2012
- [2] **F. Majdandžić:** *Uzemljivači i sustavi uzemljenja*, Graphis, 2004
- [3] **J. Nahman, I. Paunovic:** *Mesh voltages at earthing grids buried in multi-layer soil*, *Electr. Power Syst. Res.*, 2010, vol. 80, iss. 5, pp. 556–561
- [4] **I. Tolić:** *Determination of voltage conditions on the protection grounding of high voltage substations*, M.sc. Thesis, 2008
- [5] **'Power Installations Exceeding 1 kV a.c. (HD 637 S1:1999)'**, 2002
- [6] **S. Nikolovski, D. Čavlović, P. Marić, Z. Baus:** *Computer Aided Design of Power Plant Grounding System*, in '26th Scientific Conference Science to Practice', 2008
- [7] **D. Navečerel:** *Development of the model for calculation of earthing zero- sequence currents in high voltage substations*, in 'HRO Cigre', 2001, pp. 43–52
- [8] **'Pravilnik o tehničkim zahtjevima za elektroenergetska postrojenja nazivnog izmjeničnog napona iznad 1 kV (NN 105/2010)'**, 2005
- [9] **'Pravilnik o tehničkim normativima za elektroenergetska postrojenja nazivnog napona iznad 1000 V (SL. 4/74)'**, 1974
- [10] **H. Markiewicz, A. Klajn:** *Earthing Systems - Fundamentals of Calculation and Design*, Wroclav University of Technology, 2003
- [11] **T. Barić, D. Šljivac, M. Stojkov:** *Validity Limits of the Expression for Measuring soil resistivity by the Wenner method according to IEEE Standard 81-1983*, *Energija*, 2007, vol. 56, iss. 6, pp. 730–753





# MAIN TITLE OF THE PAPER SLOVENIAN TITLE

*Author<sup>1</sup>, Author<sup>2</sup>, Corresponding author<sup>✉</sup>*

Keywords: (Up to 10 keywords)

## **Abstract**

Abstract should be up to 500 words long, with no pictures, photos, equations, tables, only text.

## **Povzetek**

(Abstract in Slovenian language)

Submission of Manuscripts: All manuscripts must be submitted in English by e-mail to the editorial office at [jet@um.si](mailto:jet@um.si) to ensure fast processing. Instructions for authors are also available online at <http://www.fe.um.si/en/jet/author-instructions.html>.

Preparation of manuscripts: Manuscripts must be typed in English in prescribed journal form (MS Word editor). A MS Word template is available at the Journal Home page.

A title page consists of the main title in the English and Slovenian language; the author(s) name(s) as well as the address, affiliation, E-mail address, telephone and fax numbers of author(s). Corresponding author must be indicated.

Main title: should be centred and written with capital letters (ARIAL bold 18 pt), in first paragraph in English language, in second paragraph in Slovenian language.

Key words: A list of 3 up to 6 key words is essential for indexing purposes. (CALIBRI 10pt)

Abstract: Abstract should be up to 500 words long, with no pictures, photos, equations, tables, - text only.

Povzetek: - Abstract in Slovenian language.

Main text should be structured logically in chapters, sections and sub-sections. Type of letters is Calibri, 10pt, full justified.

---

✉ Corresponding author: Title, Name and Surname, Organisation, Department, Address, Tel.: +XXX x xxx xxx, E-mail address: x.x@xxx.xx

<sup>1</sup> Organisation, Department, Address

<sup>2</sup> Organisation, Department, Address

Units and abbreviations: Required are SI units. Abbreviations must be given in text when first mentioned.

Proofreading: The proof will be send by e-mail to the corresponding author in MS Word's Track changes function. Corresponding author is required to make their proof corrections with accepting or rejecting the tracked changes in document and answer all open comments of proof reader. The corresponding author is responsible to introduce corrections of data in the paper. The Editors are not responsible for damage or loss of submitted text. Contributors are advised to keep copies of their texts, illustrations and all other materials.

The statements, opinions and data contained in this publication are solely those of the individual authors and not of the publisher and the Editors. Neither the publisher nor the Editors can accept any legal responsibility for errors that could appear during the process.

Copyright: Submissions of a publication article implies transfer of the copyright from the author(s) to the publisher upon acceptance of the paper. Accepted papers become the permanent property of "Journal of Energy Technology". All articles published in this journal are protected by copyright, which covers the exclusive rights to reproduce and distribute the article as well as all translation rights. No material can be published without written permission of the publisher.

Chapter examples:

## 1 MAIN CHAPTER

**(Arial bold, 12pt, after paragraph 6pt space)**

### 1.1 Section

**(Arial bold, 11pt, after paragraph 6pt space)**

#### 1.1.1 Sub-section

**(Arial bold, 10pt, after paragraph 6pt space)**

Example of Equation (lined 2 cm from left margin, equation number in normal brackets (section. equation number), lined right margin, paragraph space 6pt before in after line):

$$\text{Equation} \tag{1.1}$$

Tables should have a legend that includes the title of the table at the top of the table. Each table should be cited in the text.

Table legend example:

***Table 1: Name of the table (centred, on top of the table)***

Figures and images should be labelled sequentially numbered (Arabic numbers) and cited in the text – Fig.1 or Figure 1. The legend should be below the image, picture, photo or drawing.

Figure legend example:

**Figure 1:** *Name of the figure (centred, on bottom of figure, photo, or drawing)*

## References

- [1] **N. Surname:** *Title*, Journal Title, Vol., Iss., p.p., Year of Publication
- [2] **N. Surname:** *Title*, Publisher, Year of Publication
- [3] **N. Surname:** *Title* [online], Publisher or Journal Title, Vol., Iss., p.p., Year of Publication. Available: website (date accessed)

Examples:

- [1] **J. Usenik:** *Mathematical model of the power supply system control*, Journal of Energy Technology, Vol. 2, Iss. 3, p.p. 29 – 46, 2009
- [2] **J. J. DiStefano, A.R. Stubberud, I. J. Williams:** *Theory and Problems of Feedback and Control Systems*, McGraw-Hill Book Company, 1987
- [3] **T. Žagar, L. Kegel:** *Preparation of National programme for SF and RW management taking into account the possible future evolution of ERDO* [online], Journal of Energy Technology, Vol. 9, Iss. 1, p.p. 39 – 50, 2016. Available: [http://www.fe.um.si/images/jet /Volume 9\\_Issue1/03-JET\\_marec\\_2016-PREPARATION\\_OF\\_NATIONAL.pdf](http://www.fe.um.si/images/jet /Volume 9_Issue1/03-JET_marec_2016-PREPARATION_OF_NATIONAL.pdf) (7. 10. 2016)

Example of reference-1 citation: In text [1], text continue.

## Nomenclature

(Symbols)	(Symbol meaning)
t	time



ISSN 1855-5748



9 771855 574008